Design, Integration, and Trajectory Analysis of Ramjet-Powered Projectile

By

Syed Mustafa Hassan

330637

Supervisor

Dr. Adnan Maqsood

Co-Supervisor

Dr. Raheel Nawaz

School of Interdisciplinary Engineering and Sciences

National University of Sciences and Technology

Islamabad, Pakistan

May 2023

Design, Integration, and Trajectory Analysis of Ramjet-Powered Projectile

By

Syed Mustafa Hassan

330367

A thesis submitted in partial fulfillment of the requirements for the degree of

MS Systems Engineering

Thesis Supervisor:

Dr Adnan Maqsood

Thesis Co- Supervisor:

Dr Raheel Nawaz

School of Interdisciplinary Engineering and Sciences

National University of Sciences and Technology,

Islamabad, Pakistan

May 2023

Declaration

I certify that this research work titled "*Design, Integration & Trajectory Analysis of 155 mm Ramjet – Powered Artillery Shell"* is my own work. The work has not been presented elsewhere for assessment.

I confirm that:

1. This work was done wholly or mainly while in candidature for a Master of Science degree at NUST.

2. Where any part of this thesis has been previously submitted for a degree or any other qualification at NUST or any other institution, this has been clearly stated.

3. Where I have consulted the published work of others, this is always clearly attributed.

4. Where I have quoted from the work of others, the source is always given. With the exception of such quotations, this thesis is entirely my own work.

5. I have acknowledged all main sources of help.

6. Where the thesis is based on worked done by myself jointly with others, I have made clear exactly what was done by others, and I have contributed myself.

_____

Syed Mustafa Hassan

2020-NUST-MS-SE-330367

Copyright Notice

Acknowledgments

I would like to begin by expressing my deepest gratitude to Allah, whose guidance and blessings have been instrumental in my ability to complete this thesis. I am eternally grateful for the support and love my parents have provided me throughout my academic journey, always believing in my capabilities and encouraging me to persevere.

A special mention must be made of my father, an artillery veteran whose passion and dedication to his profession have inspired me since childhood. Growing up around guns and witnessing his commitment to his work has instilled in me a deep sense of purpose, motivating me to contribute to this field by working on the topic of ramjet-powered artillery shells.

I am profoundly thankful for my work colleagues, whose camaraderie and valuable insights have enriched my learning experience. A special mention goes to my loving wife, who has been a constant source of encouragement, inspiration, and understanding, and my daughter, whose presence has brought immense joy and motivation to my life.

I would also like to express my sincere appreciation to my supervisor, Dr. Adnan Maqsood, Director of Academics, NUST, who has played a crucial role in developing my understanding of aerospace systems. His expert guidance, constructive feedback, and unwavering support have been invaluable in helping me navigate the complexities of this field. Additionally, I am deeply grateful to my co-supervisor, Dr. Raheel Nawaz, Pro Vice-Chancellor at the University of Staffordshire, UK, who is an esteemed researcher and has provided indispensable insights and guidance throughout this journey.

Furthermore, I would like to extend my heartfelt gratitude to my father-in-law, who has embraced me as his son and consistently encouraged me to become a better professional, compassionate, and responsible individual. His wisdom, love, and unwavering support have been invaluable in shaping my personal and professional growth.

Last, I am grateful to my Dr Ammar Mushtaq, Dr Mian Ilyas Ahmed, and lab engineer Hafiz Ali Haider Sehole, whose technical expertise and assistance in the lab have contributed significantly to the successful completion of my research. Their willingness to share knowledge and dedication to ensuring that the lab environment was conducive to learning have been genuinely inspiring.

In conclusion, I would like to extend my deepest gratitude to everyone who has been a part of my journey toward completing this thesis. The support, encouragement, and knowledge that each of you has shared with me have played an integral role in shaping this thesis and my growth as an individual and a researcher.

Dedicated to my beloved wife, daughter, and Family, whose tremendous support and cooperation led me to this scholastic accomplishment

ABSTRACT

This thesis presents the design, integration, and trajectory generation of a ramjet-powered 155mm projectile. The existing 155mm legacy shell is modified by increasing its length and adding rear fins for extra lift and stability. The ramjet engine was designed through an empirical framework. Aerodynamic coefficients are calculated in Missile DATCOM®. The Ramjet Engine and a look-up table of the aerodynamic coefficients were integrated into the trajectory generation model in Simulink MATLAB®. The analysis of the results indicates that the proposed design, with the integrated ramjet engine, can reach a range of over 70 km, substantially improving the legacy system. This enhanced range has significant advantages for military operations, as it allows for increased target coverage, improved accuracy, and decreased vulnerability to enemy counterattacks. Additionally, the modified artillery shell can reduce the number of rounds needed to engage targets, reducing operational costs and logistical requirements.

The main novelty of this study lies in integrating a ramjet engine with a 155mm artillery shell, which is rarely explored in the published literature due to proprietary aspects. The ramjet engine provides a sustained propulsion system that enables the artillery shell to achieve a greater range than traditional systems. This technology can potentially revolutionize the employability of artillery by providing enhanced range and accuracy for farther targets. The simulation model generates a trajectory that maximizes the range of the modified artillery shell while minimizing the impact of environmental factors such as wind and air resistance. The resulting trajectory is optimized to achieve the maximum range for the shell.

The design integration and trajectory generation process outlined in this thesis can be used as a blueprint for developing high-performance artillery shells with improved accuracy and range. The proposed design has several advantages over conventional artillery shells, including the ability to strike targets that are beyond the range of traditional artillery shells.

In summary, this study presents a novel approach to enhance the range of artillery shells by integrating a ramjet engine. The research contributes to advancing defense technology in Pakistan and provides a basis for further research in this area.

Table of Contents

List of Figures

List of Tables

List of Equations

1. Introduction

1.1 Artillery Background:

Artillery has been integral to warfare for centuries, dating back to the earliest recorded battles. The earliest artillery consisted of simple, hand-held weapons such as slingshots and spears. Over time, these primitive weapons evolved into more advanced and sophisticated systems, including cannons, mortars, and howitzers [1]. Throughout history, artillery has played a vital role in military operations by providing long-range firepower, suppression of enemy positions, and support for ground troops.

One of the most significant developments in the history of artillery was the introduction of rifled barrels in the mid-19th century. This innovation dramatically improved the accuracy and range of artillery, allowing for more effective engagement of enemy targets from greater distances. Since then, numerous advancements have been made in artillery technology, including range, accuracy, and mobility [1].

Modern artillery systems are highly advanced today, incorporating cutting-edge technologies such as GPS guidance, digital fire control systems, and advanced ammunition [2]. These systems can engage targets at ranges of several kilometers, providing a critical advantage in ground warfare.
Despite these advancements, there is room for further improvement in artillery technology. In particular, increasing the range of artillery systems remains a priority for military strategists, as it provides greater flexibility and capability on the battlefield. As such, there is a pressing need to develop new and innovative solutions to enhance the range and effectiveness of artillery systems. This is where ramjet technology in artillery shells comes in, offering the potential for a substantial increase in range and effectiveness [3].

The 155mm howitzer is a widely used artillery system, providing excellent fire support to troops on the ground [1]. However, the limitations of the traditional artillery shell have become increasingly evident, particularly in modern warfare scenarios, where longer ranges and greater

accuracy are required. Therefore, there has been a growing demand for enhanced range and accuracy in artillery systems.

To address this issue, this thesis proposes a novel approach to enhance the range of artillery shells by integrating a ramjet engine. A ramjet engine provides sustained propulsion, enabling the artillery shell to achieve a greater range than traditional systems. This technology can potentially revolutionize the employability of artillery by providing enhanced range and accuracy for farther targets.

Additionally, the trajectory generation model developed in Simulink provides a framework for optimizing the trajectory of the modified artillery shell to achieve maximum range while minimizing the impact of environmental factors. The proposed design has several advantages over conventional artillery shells, including the ability to strike targets that are beyond the range of traditional artillery shells.

1.2 Problem Statement

The existing 155mm legacy shell has limited range and accuracy, and there is a growing need for enhanced capabilities in modern warfare scenarios. Integrating a ramjet engine with an artillery shell can revolutionize the employability of artillery by providing enhanced range and accuracy for farther targets. This study explores the potential of ramjet technology for enhancing the range and accuracy of artillery systems [4].

Artillery remains one of the most effective means of delivering firepower to a designated target, and the range and accuracy of these systems are critical to their effectiveness on the battlefield. The primary motivation behind this study is rooted in the scientific and military need to enhance artillery shells' range and accuracy. Over the years, several options have been explored to enhance the range of artillery shells, including base bleed and rocket-assisted [3]. However, there is always room for improvement to address further the limitations of traditional artillery shells, which are limited in range due to lack of sustained propulsion.

The design of a ramjet-powered artillery shell with an integrated trajectory generation model is motivated by the need to overcome the limitations of traditional artillery shells. Ramjet technology provides a sustained propulsion system that enables the artillery shell to achieve a greater range than traditional systems. This technology can potentially revolutionize the employability of artillery by providing enhanced range and accuracy for farther targets.

Furthermore, the design and integration of a ramjet-powered artillery shell have practical implications for military operations [4]. With increased range and accuracy, the proposed design can reduce the number of rounds needed to engage targets, thereby reducing operational costs and logistical requirements [5]. Moreover, the extended range of the modified artillery shell allows for increased target coverage, improved accuracy, and decreased vulnerability to enemy counterattacks, which is essential for successful military operations [6].

In summary, the motivation behind this study is to design a conceptual model of a ramjet-integrated artillery shell and its trajectory generation that overcomes the limitations of traditional artillery shells. The proposed design has significant potential for improving the range and accuracy of artillery systems, which has practical implications for military operations.

1.3 Research Objective

The main objective of this study is to design, integrate and generate the trajectory of a ramjet-powered 155mm artillery shell. The study aims to explore the potential of ramjet technology for enhancing the range and accuracy of artillery systems. The specific research objectives are:

1. To modify the existing 155mm legacy shell by increasing its length and adding rear fins for extra lift and stability.
2. To calculate the aerodynamic coefficients using Missile Datcom.
3. To mathematically design a ramjet engine in MathCAD that can be integrated with the modified artillery shell.
4. To integrate the ramjet engine and the aerodynamic coefficients as a look-up table into the trajectory generation model in SIMULINK Matlab.
5. To analyze the results of the trajectory generation and determine the range enhancement achieved by the modified artillery shell.

1.4 Contribution

The contribution of this thesis lies in developing a novel approach to enhance the range of artillery shells through the integration of a ramjet engine. This study provides a conceptual design and integration process of a ramjet-powered 155mm artillery shell, a unique and innovative technology for artillery systems.

Integrating a ramjet engine with artillery shells can revolutionize the employability of artillery by providing enhanced range and accuracy for farther targets. This could significantly improve the effectiveness of military operations and reduce the need for additional resources. This research contributes to advancing military technology and provides a basis for further research.

The development of high-performance artillery shells with improved accuracy and range could be beneficial in modern Artillery weapons. Integrating ramjet technology with other systems could enhance performance, leading to more efficient and effective operations. Moreover, this research could have broader applications beyond 155 calibers only.

In summary, the contributions of this thesis can be outlined as follows:

1. Development of a 155mm ramjet engine and its integration with the existing legacy-based artillery shells
2. Trajectory generation model for optimizing the range of the modified artillery shell
3. Advancement of military technology through the integration of a ramjet engine with artillery shells
4. Potential for broader applications of ramjet technology beyond 155mm calibers only

The findings of this study could have significant implications for the future of artillery systems and could pave the way for the development of other high-performance weapons systems.

2. Literature Review

2.1 Base Bleed

2.1.1 Introduction

Extended-range-munitions (ERM) are crucial in military operations by allowing projectiles to reach targets at greater distances. Predicting the performance of ERM is essential for optimizing their effectiveness. In recent studies, researchers have explored various approaches to understanding and enhancing the performance of ERM, mainly through the use of base bleed units. This literature review will examine different research studies that investigate the impact of base bleed units on ERM performance and explore optimization techniques for achieving drag reduction and increased range. The review will provide a comprehensive overview of the findings and contributions of these studies.

Lemos et al. [7] proposed a holistic approach to predict the performance of extended-range munitions by integrating aerodynamic, internal ballistics, and trajectory effects. The study combined chemical composition data, bench tests, combustion simulations, aerodynamic simulations, and trajectory dynamics simulations to estimate the behavior of a Base Bleed (BB) unit. The research findings emphasized [7] integrating various aspects of ERM performance. Lemos et al. contributed a valuable approach to understanding and predicting the behavior of ERM and the impact of base bleed chemistry on ballistic performance.

De and Chettri [8] studied optimizing bleed projectile design using computational analysis. The study aimed to reduce drag and increase the range of artillery guns, particularly in challenging terrains. The researchers aimed to validate and computationally alter the ammunition design to reduce drag while maintaining lethality and compatibility with existing artillery guns as shown in figure 1 below. The study primarily focused on the exterior ballistics of a 155 mm M864 artillery shell and examined the effects of base bleed and boat-tail angle on drag reduction. Through computational analysis, the researchers achieved significant drag reduction and demonstrated the potential for increasing the range of artillery projectiles [8].

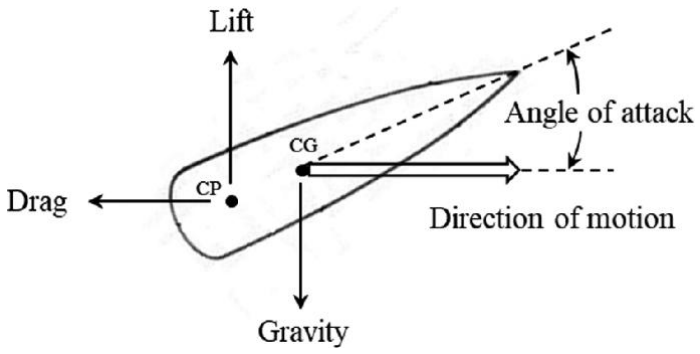

Figure 1: Drag Reduction with Optimum Designing of a Base Bleed Projectile Using Computational Analysis[8]

2.1.4 Base Bleed Effect and Research Approaches

Base bleed units are an active method for increasing the range of artillery projectiles by reducing base drag, resulting in an extended range [7]. Numerous researchers have investigated the base bleed effect using various research approaches, including firing tests, wind tunnel experiments, analytical methods, and computational fluid dynamics simulations. The primary focus of these studies has been to explore the impact of flow parameters and base ejection configurations on drag reduction [9]. The studies have utilized different types of gases and propellants to achieve base bleeds, such as solid propellants, air, argon, hydrogen, and helium.

2.1.5 Base Bleed Grain Dimensions and Performance

To maximize the range extension of a base bleed projectile, optimizing the dimensions of the base bleed grain is crucial [9]. The configuration of the base bleed grain, such as a tubular, slotted tubular cylinder, or donut shape, has been extensively studied as shown in figure 2 below. The grains are typically divided into two or three equal parts by 2 or 3 slots [11]. The slotted tubular cylinder or donut shape is the most commonly employed configuration.

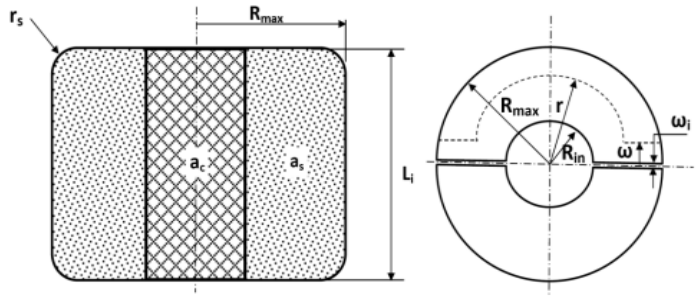

Figure 2: Geometry of the base bleed grain[11]

Several factors come into play when considering optimizing base bleed grain dimensions. Firstly, ballistic performance requirements must be considered to ensure the desired range extension while maintaining the necessary lethality of the projectile. Secondly, design constraints related to material strength and aerodynamics play a significant role in determining the dimensions of the base bleed grain. It is essential to consider the structural integrity of the projectile and its ability to withstand the forces and pressures experienced during flight. Additionally, the maximum pressure inside the barrel that affects the projectile base must be considered during the design process [9]. Studies have demonstrated that base drag reduction through base bleeding is most efficient at high supersonic velocities of artillery projectiles [10]. This implies that the base bleed unit performs optimally during the initial few seconds of projectile flight after leaving the barrel muzzle as shown in figure 3 below. To achieve the maximum range, the base bleed grain should generate a relatively large mass flow rate and attain the optimal value of the injection parameter during the early supersonic phase of flight.

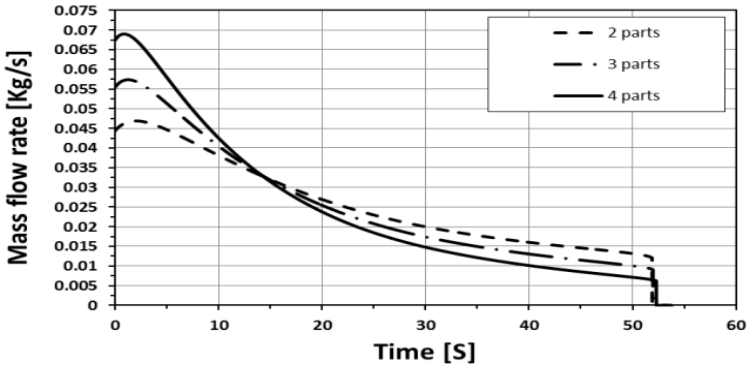

Figure 3: Predicted mass flow rate time history in case of different numbers of base bleed grains[10].

Computational work conducted by Ref. [10] has shown that the increase in base pressure due to the base bleed unit is directly proportional to the projectile's flying velocity. Consequently, higher base bleeds projectile speeds at the same injection parameter result in elevated base pressure [9]. Therefore, studying the effect of base bleed grain dimensions on the ballistic performance of artillery projectiles becomes crucial when designing a rocket-assisted unit. It is necessary to optimize the dimensions of the grains to prevent interference between units while achieving maximum range without significantly reducing projectile lethality [9].

In the study conducted by Abou-Elela et al. [9], the authors investigated the effect of the main dimensions of the base bleed grain through an analytical model. The study considered the grain's length, inner diameter, and maximum diameter. Additionally, the impact of the base bleed exit diameter was examined, and a new method for controlling the mass flow rate and injection parameters using a deformable exit diameter was proposed. The study applied these findings to a base bleed projectile model, specifically the K307 model, launched with a muzzle velocity of 910 m/s at an angle of fire of 51.2°, corresponding to the maximum range scenario [9].

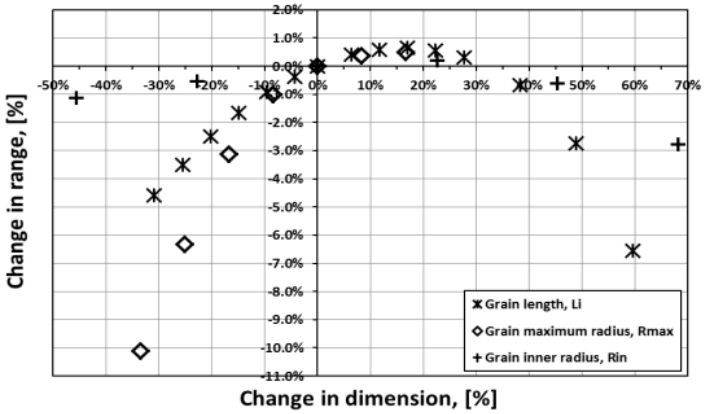

Figure 4: Predicted effects of base bleed grain dimensions change on a range[9]

The base bleeds grain in the Abou-Elela et al. study consisted of two identical solid propellant grains as shown in figure 4 above. The burning surfaces of the grains comprised an inner cylinder and four flat surfaces separated by a 3 mm slot (ωi). During launch, the slots were held open by four spacers, while the remaining grain surfaces were covered by an inhibitor [9].

The study's findings revealed the importance of optimizing the dimensions of the base bleed grain for achieving desirable ballistic performance. Through the analytical model, Abou-Elela et al. provided insights into the impact of grain length, inner diameter, and maximum diameter on the performance of artillery projectiles equipped with base bleed units. Furthermore, the proposed method of using a deformable exit diameter showed promise in controlling the mass flow rate and injection parameters [9].

Abou-Elela et al. [10] comprehensively analyzed the ballistic performance of a 155mm K307 extended-range projectile equipped with a base bleed unit. Through analytical modeling and computational resources, the authors examined the influence of parameters such as burning rate, number of base bleed grain parts, and grain dimensions on base bleed performance. Their findings revealed that improved ballistic performance could be achieved by ensuring a relatively large exit mass flow rate of burnt gases during the initial stages of projectile flight as shown in figure 5 below [10].

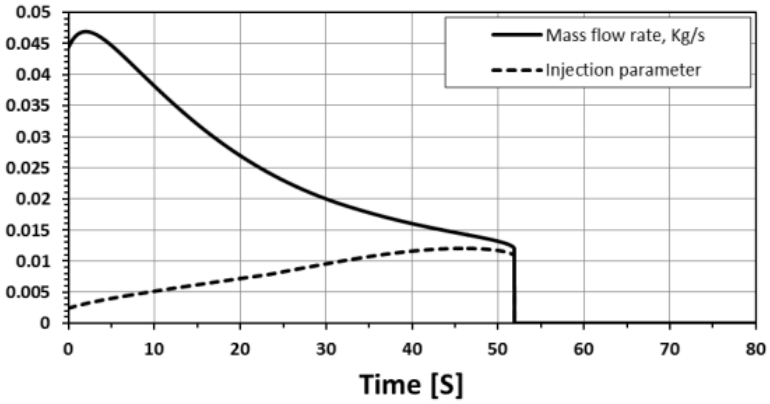

Figure 5: Predicted time history of mass flow rate and the ignition parameter [10]

Abou-Elela et al. [10] introduced a novel technique involving a multi-burn rate grain in the base bleed unit to modify the mass flow rate along the trajectory. They achieved an extended projectile range by filling the base bleed unit with a grain that burns at two different rates.

Computational Fluid Dynamics (CFD) and the commercial code PRODAS were employed to investigate the effect of the base bleed unit, both when activated and deactivated, on the projectile

trajectory [10]. The authors also examined the impact of changing the main dimensions of the base bleed grain as shown in figure 6 below.

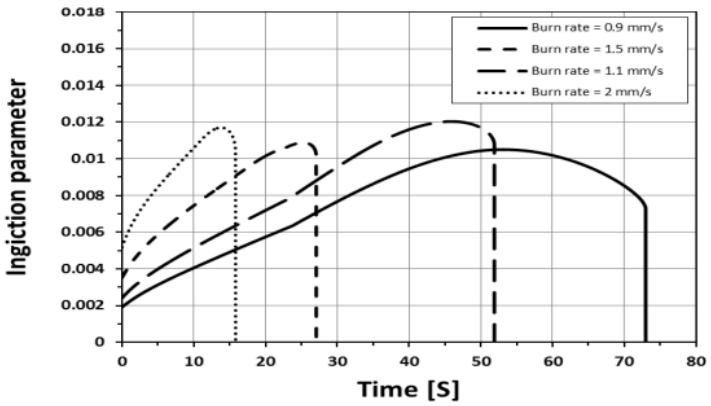

Figure 6: Predicted time history of injection parameter for different burn rates [10]

2.1.7 Projectile Base Configuration and Base Bleed Orifice

The configuration of the projectile base and the design of the base bleed orifice significantly influence the performance of the base bleed unit. These factors affect the interaction between the ejected gases and the free-stream air passing the projectile base [11]. Various research studies have utilized computational capabilities, such as CFD, and experimental facilities to investigate these parameters [11]. The aim is to understand their impact on base bleed performance and optimize the design accordingly.

2.1.8 Base Bleed Drag Reduction Model

A base bleed drag reduction model was introduced by Nils R. Gurnners [12], which enables the calculation of trajectory and performance of base bleed projectiles, considering the effect of projectile spin. This model demonstrated a good agreement between predicted results and experimental data, providing a valuable tool for evaluating the performance of base bleed units.

2.1.9 Effect of Spinning Rate on Burning Rate of Solid Propellant

The burning rate of the base bleed grain surfaces, such as cylindrical and slots, is affected by the spinning rate of the projectile [13]. J. Danberg et al. conducted an experimental study to analyze the relationship between the spinning and burning rates, specifically for the M864 base bleed

projectile [13]. The results were utilized to formulate an equation that expresses the effect of spin on the burn rate of base bleed grain surfaces in trajectory models.

2.1.10 Effect of Injection Parameter on Drag Reduction

The injection parameter is crucial in optimizing the performance of base bleed units. Numerous researchers have investigated the effect of the injection parameter on drag reduction for different Mach regions and various gases [15] [16] [17]. These studies have shown that drag reduction increases with an increase in the injection parameter up to an optimum value, which depends on factors such as the type of ejected gases, ejection configuration, and free stream conditions [12].

2.1.11 Model for Predicting Drag Reduction of Base Bleed Projectiles

Jun-Silk Hwang et al. developed a model to predict the drag reduction of base bleed projectiles at various velocities [14]. The study aimed to determine the optimum burning rate for the maximum projectile range. The results demonstrated that the optimal burning rate ranged from 1.1 to 1.3 mm/s for velocities between 810 and 910 m/s [14]. This information provides valuable insights for designing base bleed units that achieve optimal drag reduction and extended range.

2.1.12 Experimental Firing Study to Improve Base Bleed Projectile Performance

An experimental firing study was conducted to enhance the performance of base bleed projectiles [15]. The study focused on three aspects: the burnt surface area of the base bleed grain by altering the number of slots, the burning rate of the base bleed grain composition, and the optimization of the base geometry. The study improved projectiles' performance through careful adjustments, equipped with base bleed units that featured a grain with three slots [15]. These findings contribute to the ongoing efforts to enhance base bleed technology.

2.1.13 Development of a C++ Code for Predicting Trajectory Parameters

A semi-analytical model was developed using a C++ code to predict the trajectory parameters of the base bleed projectile K307 [14]. This model enables examining the effect of changing burning rate and grain geometry on the projectile's range. Analyzing these parameters introduced a new

technique to achieve a proper mass flow along the trajectory [10]. The development of this model provides a valuable tool for optimizing base bleed units and predicting their performance.

2.1.14 Study on the Effect of Changing Burning Rate and Grain Geometry on Range

Using the developed semi-analytical model, researchers conducted a study on the effect of changing the burning rate and grain geometry on the range of the base bleed projectile [14]. This investigation aimed to identify the optimal parameters leading to extended-range performance. By analyzing the results, researchers gained insights into the relationship between burning rate, grain geometry, and range, contributing to the ongoing advancements in base bleed technology.

2.1.15 Introduction of a New Technique for Proper Mass Flow along the Trajectory

By examining various parameters using the developed C++ code, researchers introduced a new technique to ensure a proper mass flow along the trajectory of the base bleed projectile [10]. This technique offers a means of optimizing the mass flow rate of burnt gases at different stages of the projectile's flight, thereby enhancing the overall performance and range. Introducing this technique represents a significant advancement in base bleed technology.

2.1.16 Optimizing Base Bleed Grain Parameters for Enhanced Ballistic Performance of Long-Range Artillery

Long-range artillery plays a crucial role in modern warfare, and researchers continually strive to enhance the range of projectiles. One of the primary concerns in achieving extended range is reducing base drag, which accounts for over 50% of the total drag experienced by projectiles at transonic and supersonic speeds [16]. Base bleeding, which involves injecting hot burnt gases behind the projectile base, effectively mitigates base drag by increasing the wake region pressure [16].

Despite previous research exploring the impact of base bleed grain parameters on ballistic performance, these studies often analyzed each parameter separately, and there was a lack of focus on optimizing the dimensions of the base bleed grain [16]. In this context, Abou-Elela et al. conducted a study presented at the 16th International Conference on Aerospace Sciences &

Aviation Technology (ASAT-16) to optimize base bleed grain parameters for maximum ballistic performance [16]. Their investigation considered design variables such as outer radius, inner radius, length, burn rate, and base bleed unit orifice diameter while exploring the innovative concept of a multi-burn rate base bleed grain as shown in table 1 below [16].

Optimization Case study designation	**Base Bleed studying variables upper and lower limit**					**No of Slots**
	Outer Radius	**Inner Radius**	**Length**	**Exit diameter**	**Burn Rate**	
	R_{max}, [mm]	**R_{in}, [mm]**	**L_i, [mm]**	**D_{exit}, [mm]**	**BR1, [mm/s]**	**Ns**
Case#1, PBB 1	60	20	94	44	1.1	2-3-4
Case#1, PBB 2	60	20	94	44	0.9-1.5	
Case#1, PBB 3	60	18-27	94	40-56	0.9-1.3	
Case#1, PBB 4	40 - 70	18-27	75-135	40-56	0.9-1.3	

Table 1: Studied cases of the original base bleed grain, upper and lower constraints of each design variable[16].

2.1.17 Optimization Study of Base Bleed Grain Parameters

Abou-Elela et al. [16] developed a comprehensive analytical model in a C++ environment to accurately evaluate the range of projectiles. To achieve optimization, the researchers employed the Design of Experiments (DOE) technique and the Response Surface Method (RSM) to construct a smooth response function that served as the objective function in the design optimization formulation [16]. This approach allowed for identifying design variables that contributed to the maximum range.

2.1.18 Analytical Modeling and Optimization Process

The developed C++ model, DOE, and RSM were central in optimizing base bleed grain parameters [16]. Using the validated C++ model, the researchers calculated the projectile range, which served as the primary metric for evaluating the performance of different parameter combinations [16].

The study by Abou-Elela et al. [16] yielded essential insights into optimizing base bleed grain parameters and its impact on ballistic performance. The findings emphasized optimization's significance in enhancing base bleed projectiles' performance. The researchers presented the optimized values for each parameter, showcasing the specific parameter combinations that resulted in the maximum range [16]. Furthermore, applying the multi-burn rate base bleed concept demonstrated a significant increase in range across all cases, with improvements of up to 12% compared to the original base bleed grain [16].

2.1.19 Optimization of Low Signature Base Bleed Propellant Formulations for Enhanced Performance and Reduced Smoke Emissions in Artillery Projectiles

Artillery projectiles with extended ranges are of great importance in modern warfare. One effective method to increase range is using base bleed (BB) units, which reduce base drag and improve projectile performance [17]. However, generating secondary smoke while burning base bleed compositions remains a concern, as it can aid in detecting the projectile [17]. Optimizing low signature base bleed propellant formulations aims to minimize secondary smoke while maintaining high impulse and low flame temperature [17].

2.1.20 Base Bleed Propellant Formulations and Their Characteristics

Composite base bleed propellant formulations have various components influencing their properties and performance [18, 19]. These formulations aim to achieve propellants with high mechanical properties and low burning rates [16, 22]. Parameters such as solid component quantities, binder type, curing agent, particle size distributions, and bonding agents play crucial roles as shown in figure 7 below [18, 19].

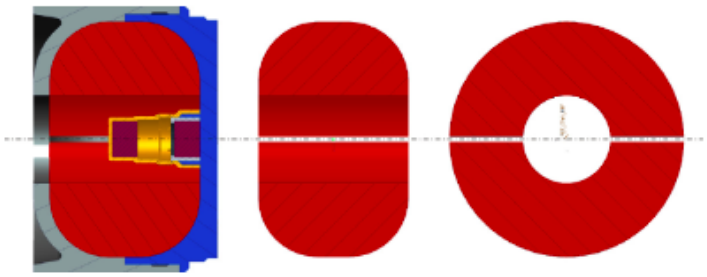

Figure 7: Scheme of gas generator unit and propellant grain[18]

2.1.21 Drawbacks of Base Bleed Propellants: Smoke Signature

One drawback of base bleed propellants is the production of primary and secondary smoke during burning. This smoke can increase the detectability of the projectile during its flight toward the target. To address this issue, researchers have explored the development of "clean burning propellants" that minimize smoke emissions by eliminating chlorine as an ingredient [20]. Various chemical additives, including magnesium (Mg) powder and hexahydro-1,3,5-trinitro-1,3,5-triazine (RDX), have been investigated to reduce smoke emissions.

2.1.22 Optimization of Low Signature Base Bleed Propellant Formulations

Ehab M. Youssef et al. conducted a study to optimize low signature base bleed propellant formulations [17]. The optimization process involved intensive ICT formulation results and the utilization of design expert software [17]. This process obtained two base bleed propellant formulations: one with a 10.27% RDX/AP ratio and another with a 7.02% Mg/AP ratio [17]. Experimental testing demonstrated a reduction in secondary smoke values by 16% and 55% for the RDX/AP and Mg/AP ratios, respectively, compared to the baseline BB reference composition [17].

2.1.23 Properties and Performance of Optimized Formulations

The optimized compositions were further analyzed to determine their density, heat of the explosion, ignition temperature, maximum stress, strain, and burning rate [17]. The NR7 composition containing 7% RDX increased maximum stress and strain values by 7% and 27%, respectively, while the burning rate decreased by 14% [17]. On the other hand, the NM5 composition containing 5% Mg showed a 15% increase in maximum stress, a slight decrease in strain (6%), and a 20% increase in the burning rate [17]. Both compositions met the required properties for base bleed applications, with significant reductions in secondary smoke emissions [17].

2.2 Rocket-Assisted Projectile

2.2.1 Introduction

Rocket-assisted projectiles (RAPs) have emerged as a promising technology in artillery systems, offering an extended range and enhanced performance over traditional projectiles. This literature review delves into the current research on RAPs, focusing on three crucial aspects: safety concerns, performance enhancement, and design optimization. The studies covered in this review provide valuable insights into the development and potential of RAPs in the military sector.

2.2.2 Safety Testing of Rocket-Assisted Projectiles

Tozer [21] carried out an extensive safety testing program on 5-inch 38-caliber RAPs, encompassing a range of tests, such as impact, vibration, and thermal tests. The results demonstrated that RAPs could be safely handled, stored, and fired without introducing any unusual hazards for the crew or the environment. Although the bullet impact tests did not fully satisfy the passing criteria as shown in figure 8 below, RAPs were no more hazardous than conventional in-service projectiles, indicating their safe deployment in artillery systems [21].

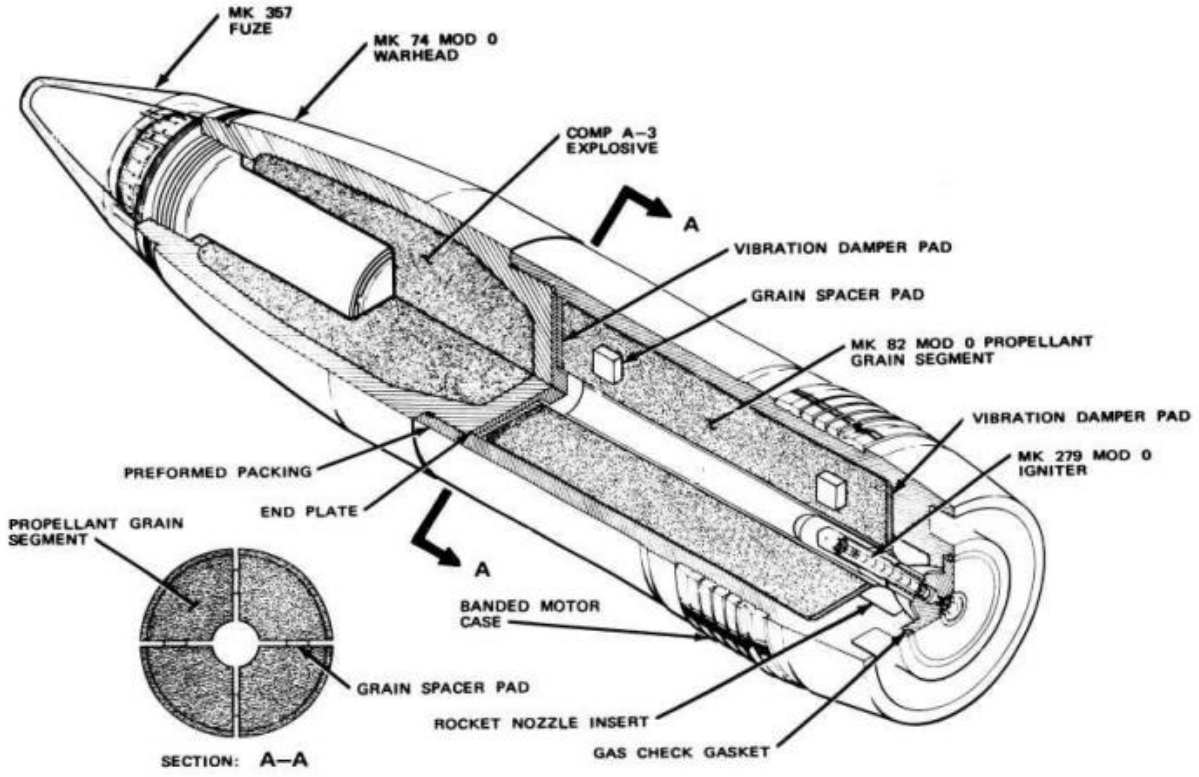

Figure 8: Mk 57 Mod O RAP[21]

2.2.3 Enhancing the Performance of Rocket-Assisted Projectiles

Kim et al. [22] investigated the ballistic performance of various solid rocket fuels and shell designs for 120 mm RAPs, emphasizing maximizing the range and stability. Through the comparative analysis of different designs, one of the tested models demonstrated a substantial increase in range - a remarkable 70% improvement compared to conventional projectiles. This model achieved a

maximum range of 14.5 km, which is a significant development in the performance of artillery systems [22].

2.2.4 Optimizing the Design of Rocket-Assisted Projectiles

Arkhipov and Perfilieva [23] proposed a comprehensive methodology for optimizing the design of RAPs, considering various factors such as aerodynamic drag, structural integrity, and propulsion systems. They developed an advanced numerical model that enabled them to predict the optimal design parameters for RAPs, considering the specific requirements of different military scenarios. This optimization process resulted in the development of more efficient and reliable RAPs, paving the way for their broader adoption in modern artillery systems as hown in figure 9 below [23].

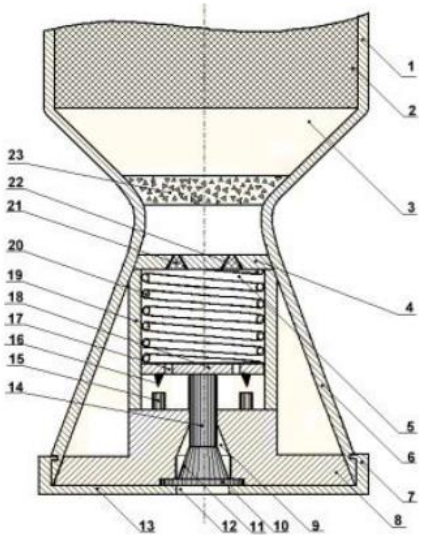

Figure 9: The Scheme of the rocket motor rocket-assisted projectile[23]

2.2.5 Polyurethane-based Composite Solid Propellants for RAPs

Recent research has shifted focus towards solid propellant rocket motors to extend the range of large caliber ammunition gun systems [24]. Rocket-assisted projectiles (RAPs), both fin and spin-stabilized, are subjected to high acceleration and centrifugal forces during launch, which requires solid rocket propellants with high tensile strength, flexibility, and ultimate tensile strain limits [25]. A key objective for RAP designers is to create a propellant grain that fulfills the required thrust-time schedule for range extension while maintaining mechanical properties [26]. Polyurethanes

(PUs) are a versatile class of polymers that can be used as binders in solid propellants due to their tailorable properties [27, 28]. The mechanical characteristics and ballistic performance of polyurethane-based composite solid propellants are influenced by various factors, including the synthesis process, binder variation, propellant mixture content, and motor manufacturing conditions [29] [30] [31] [32] [33] [34] [35] [36] [37].

2.2.6 Challenges and Future Prospects of Rocket-Assisted Projectiles

Despite the advancements in RAP technology, challenges still need to be addressed to improve their overall effectiveness and integration into artillery systems. For instance, the accuracy of RAPs at extended ranges remains a critical concern, as longer-range projectiles are more susceptible to wind and atmospheric effects, which can impact their trajectory [24]. Developing cost-effective manufacturing processes for RAPs is also essential to make them a viable option for wide-scale deployment. Exploring the mechanical characteristics and ballistic performance of polyurethane-based composite solid propellants and investigating the correlations between these properties contribute to addressing these challenges [37].

2.2.7 Concluding Remarks

Rocket-assisted projectiles have demonstrated their potential to significantly extend the range and enhance the performance of artillery systems. While advancements in safety testing, performance enhancement, and design optimization have been made, addressing the remaining challenges, such as accuracy and manufacturing costs, will further solidify RAPs' role in modern military applications. Research into polyurethane-based composite solid propellants has revealed promising avenues for improving RAP technology, highlighting the importance of understanding these propellants' mechanical properties and ballistic performance in achieving mission objectives. As research and development continue, RAPs are expected to become an increasingly important component of artillery systems, providing an edge to military forces in various combat scenarios.

2.3 Ramjet Powered Artillery

2.3.1 Introduction

The rapid advancement of military and aerospace technology has increasingly emphasized the development of efficient and high-performance propulsion systems. Among these propulsion systems, solid fuel ramjet (SFRJ) and solid fuel scramjet (SFSJ) engines have emerged as promising solutions for applications such as extended-range artillery, hypersonic vehicles, and other aerospace applications. These engines offer the potential for improved efficiency, increased range, and higher payload capacity compared to conventional propulsion systems.

This literature review will overview recent advancements and ongoing research in solid-fuel ramjet and solid-fuel scramjet engine technologies. Specifically, the review will focus on the propulsion systems' design, optimization, performance evaluation, and their applications in artillery systems and hypersonic vehicles. Additionally, the review will discuss the development of novel fuel sources and materials to enhance the performance of these engines, as well as the challenges and future research directions in this field.

The review is organized into eight sections, beginning with an introduction to the topic, followed by discussions on enhancing artillery systems performance, long-range artillery projectiles with rocket ramjets, combined solid rocket/scramjet engines, and solid fuel-rich propellants for ramjet applications. Subsequent sections will cover gun-launched ramjet-propelled artillery shells, future research directions, and concluding remarks.

Through a comprehensive examination of these studies, this literature review provides valuable insights into the current state of solid fuel ramjet and solid fuel scramjet engine technologies, their potential applications, and the future research necessary to further advance these propulsion systems for military and aerospace applications.

2.3.2 Gun-Launched Ramjet Propelled Artillery Shells

Kanga et al. [38] conducted a study aiming to design a 155 mm gun-launched ramjet-propelled artillery shell to achieve a range of over 80 km. The research focused on maximizing the high explosive volume and the specific impulse of the ramjet engine as shown in figure 10 below. The results of this study highlighted the potential of gun-launched ramjet-propelled artillery shells to extend the range of 155 mm howitzer systems significantly. The adoption of SFRJ engines in artillery projectiles can lead to a new generation of extended-range artillery, meeting the demands of modern military operations.

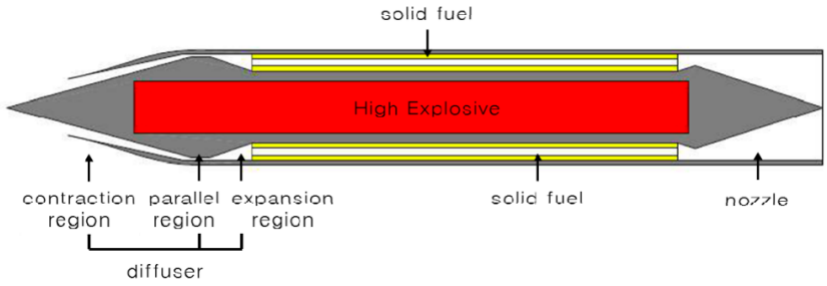

Figure 10: 155 mm gun-launched ramjet-propelled artillery shell[38]

Future research should refine the shape derived from this study using computational fluid dynamics (CFD) calculations considering viscosity [38]. These improvements can potentially enhance the performance of the gun-launched ramjet-propelled artillery shell, allowing for even greater range extensions and more effective use of the high explosive volume as shown in figure 11 below. The development of such projectiles has the potential to revolutionize artillery systems by providing unprecedented range capabilities, meeting the evolving demands of modern warfare.

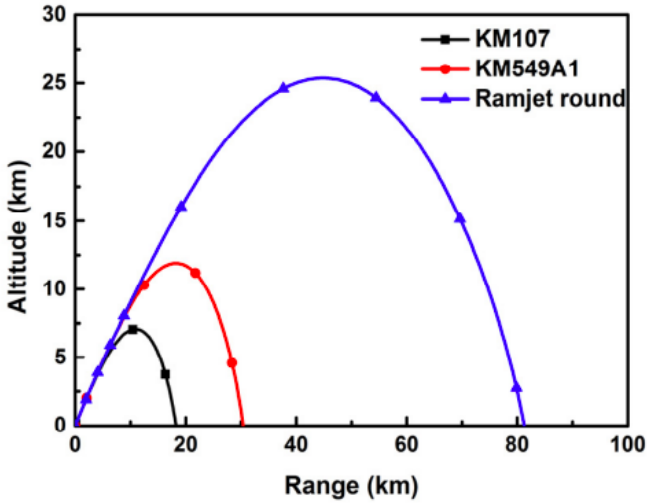

Figure 11: Trajectory of typical artillery shells and gun-launched ramjet-propelled artillery shell[38]

2.3.3 Solid-Fuel Scramjet Combustors

Wang et al. [39] studied solid-fuel scramjet combustors, examining the specific thrust change rule throughout the working process using numerical and experimental methods. The researchers designed and constructed a methane-burning vitiated air heater to accurately simulate the flight environment at Mach 6 and an altitude of 25 km. They developed a novel quasi-one-dimensional numerical method based on the two-dimensional numerical flow field results, simplifying unsteady combustion and flow in solid-fuel scramjets. The study provided valuable insights into the behavior of solid-fuel scramjet combustors under different conditions, contributing to the ongoing research in this field.

2.3.3 Numerical Analysis of Solid Fuel Scramjet Operating at Mach 4 to 6

Biao et al. [40] conducted numerical simulations to analyze the performance of solid fuel scramjet (SFSCRJ) operating at Mach 4 to. Their primary objective is to explore the feasibility of low takeover speed for SFSCRJ. The researchers developed a numerical model based on prior experiments and incorporated a constant area isolator before the combustor. The isolator changed the airflow to subsonic and returned it to supersonic in the diverging section at the Mach 4 condition. The results indicated the feasibility of SFSCRJ operating at low-flight Mach. The performance of the combustor improved as the inflow static pressure increased. Still, there was a tradeoff between the enhanced combustor performance and the increased total pressure loss in the

inlet [40]. This study contributes valuable insights into the effects of various conditions on SFSCRJ performance, aiding further research and development in this area.

2.3.4 Long-Range Artillery Projectiles with Rocket Ramjets

Kert et al. [41] recently explored the potential of developing long-range artillery projectiles with rocket ramjets to increase the firing range to 60 km or more. They designed promising structural designs for ammunition with rocket ramjets of 130, 152, and 203 mm caliber based on analyzing existing technical solutions. The authors implemented mathematical models of the ballistic functioning of artillery projectiles in software, allowing for the analysis of the influence of design parameters on the ballistic functioning of active, active-reactive ammunition and ammunition with rocket ramjets. Their study concluded that it is possible and advisable to develop long-range projectiles equipped with an out-barrel dispersal system, including rocket ramjets on paste fuel, with or without solid propellant ramjets [41]. This work contributes to the ongoing efforts in artillery technology to enhance artillery projectiles' firing range and efficiency, complementing other research in the field.

2.3.5 Past Attempts and Developments

Various attempts have been made to increase artillery projectiles' firing range and efficiency, creating several prototype ammunition samples. In recent years, several domestic patents have been granted for artillery projectiles with ramjet and solid rocket-ramjet engines as shown in figure 12,13 and 14 below [42, 43, 44].

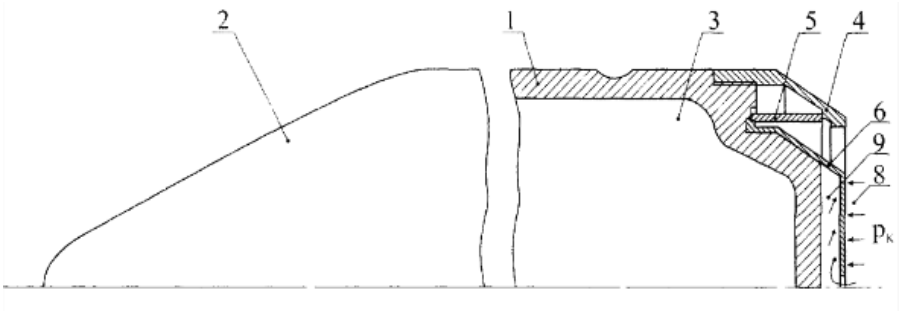

Figure 12: RU 2251068 C1[42]

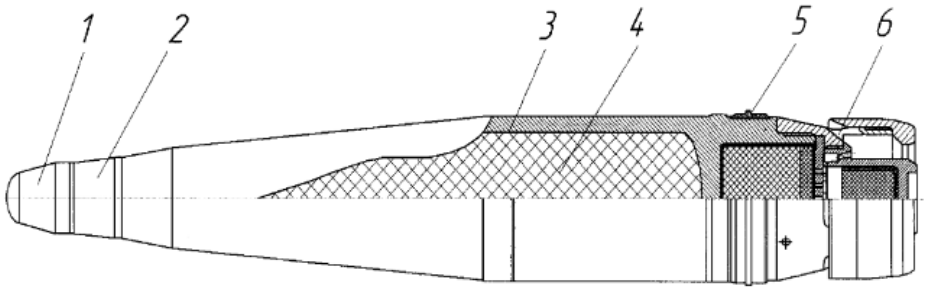

Figure 13: RU 2493533 C1[43]

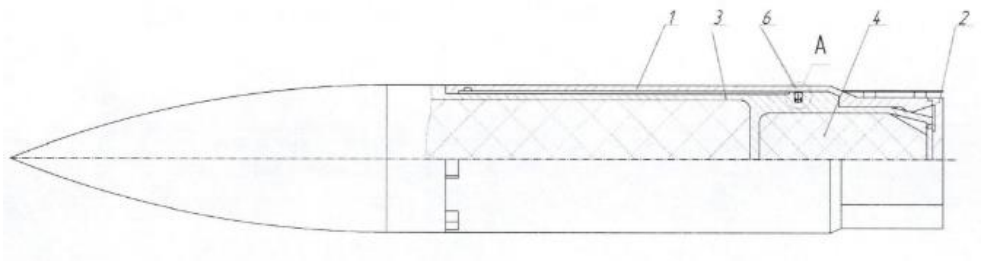

Figure 14: RU 2486452 C1[44]

Internationally, similar developments are taking place, such as the Israeli firm Somchem's independent development of the 155mm active-reactive projectile PRO-RAM with a rocket-ramjet engine, a variant of the M2005 VLAP projectile. According to the developers, the firing range of this projectile from a gun with a barrel length of 52 calibers will be at least 70 km.

2.3.6 High-Energy Paste-Like Fuel Compositions

The development of high-energy paste-like fuel compositions in recent years has made it possible to implement effective solid-fuel rocket-ramjet engines for artillery projectiles [45, 46]. The studies have shown the potential and feasibility of developing long-range projectiles equipped with an out-barrel acceleration system consisting of either a combination of solid rocket engines or solid propellant ramjets with solid fuel rocket-ramjet engines, or only solid fuel rocket-ramjet engines [41]. The appropriate range of such projectiles must be determined through corresponding military-scientific research.

2.3.7 Dispersion Mitigation Techniques

Dispersion, which refers to the significant deviation in projectile trajectories when firing unguided artillery projectiles at long ranges, poses a challenge to the effectiveness and accuracy of long-range artillery. To address this issue, researchers have proposed various trajectory correction methods [41]. These methods can be categorized into two main types: impulsive and aerodynamic. Impulsive correction techniques involve applying short bursts of force to the projectile during its flight, altering its trajectory in a controlled manner. These techniques may involve small solid rocket motors, which can be activated at specific points during the projectile's flight to achieve the desired corrections.

Aerodynamic correction techniques, on the other hand, rely on manipulating the aerodynamic forces acting on the projectile to adjust its trajectory. This can be achieved through movable control surfaces or other aerodynamic devices that can change the projectile's aerodynamic properties during flight. These alterations can effectively reduce dispersion and increase the accuracy and efficiency of long-range artillery projectiles.

Both impulsive and aerodynamic correction methods have their advantages and challenges. Further research is necessary to determine the most suitable approach for specific applications and to optimize these techniques to enhance the overall performance of long-range artillery projectiles.

2.3.8 Combined Solid Rocket/Scramjet Engines

He et al. [47] introduced a novel propulsion system called the solid rocket/scramjet combined engine, which utilizes fuel-rich solid propellant as its fuel. The combustion process takes place in the gas generator, producing primary gas. This primary gas is subsequently injected into the supersonic secondary combustor, where afterburning occurs. Finally, the secondary gas is expelled from the nozzle, generating thrust. The researchers conducted a theoretical analysis to obtain evaluation indexes characterized by the fuel.

He et al. [47] proposed a novel propulsion system known as the solid rocket/scramjet combined engine, which leverages fuel-rich solid propellant as its primary fuel source. The combustion

process occurs in a gas generator, producing a primary gas. This primary gas is injected into a supersonic secondary combustor, where afterburning occurs. Finally, the secondary gas is expelled through a nozzle, generating thrust.

2.3.9 Theoretical Analysis and Performance Evaluation

The researchers conducted a theoretical analysis to establish evaluation indices characterized by the fuel's calorific value, theoretical air requirement, and density. The analysis demonstrated the combined engine's advantages in acceleration ability and flight range [47]. Utilizing the Navier-Stokes Equations, k-ε turbulence model, and Eddy Dissipation combustion model, He et al. simulated the three-dimensional supersonic combustion flow field to study the engine's performance. Their results indicated that the primary gas could be reliably ignited in the secondary combustor, and the supersonic combustion efficiency reached 82%. This confirmed the feasibility of the proposed combustion organization method.

To quantitatively evaluate the performance of this new type of engine, the authors developed a systematic method based on the principles of mass conservation, energy conservation, and momentum conservation. The analysis revealed that the specific impulse of the solid rocket/scramjet combined engine is 2-3 times that of traditional solid rocket motors, suggesting that it could become a high-performance propulsion system for future hypersonic technology applications [47].

2.3.10 Introduction to Fuel-Rich Propellants

In recent years, the development of solid fuel-rich propellants for use in ramjets has become a promising avenue for the active propulsion of artillery shells, such as the 155 mm artillery shell as shown in figure 15 below. Velari et al. [48] conducted an extensive study on fuel-rich propellants of aluminum, ammonium perchlorate, and hydroxyl-terminated polybutadiene (HTPB).

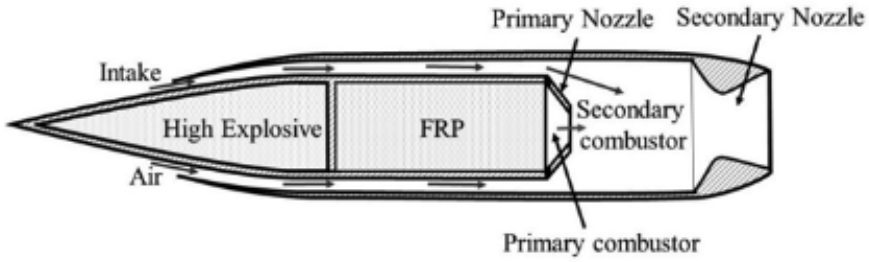

Figure 15: Schematic of artillery shell with ramjet n fuel-rich mode[48]

Their research aimed to enhance the burn rates of the propellant, providing the necessary burn rates at the lowest possible pressures in the primary combustor of the ramjet. The propellant selection was based on the working time period of the base bleed unit to calculate the required burn rate and corresponding pressure in the primary combustor as shown in figure 16 below.

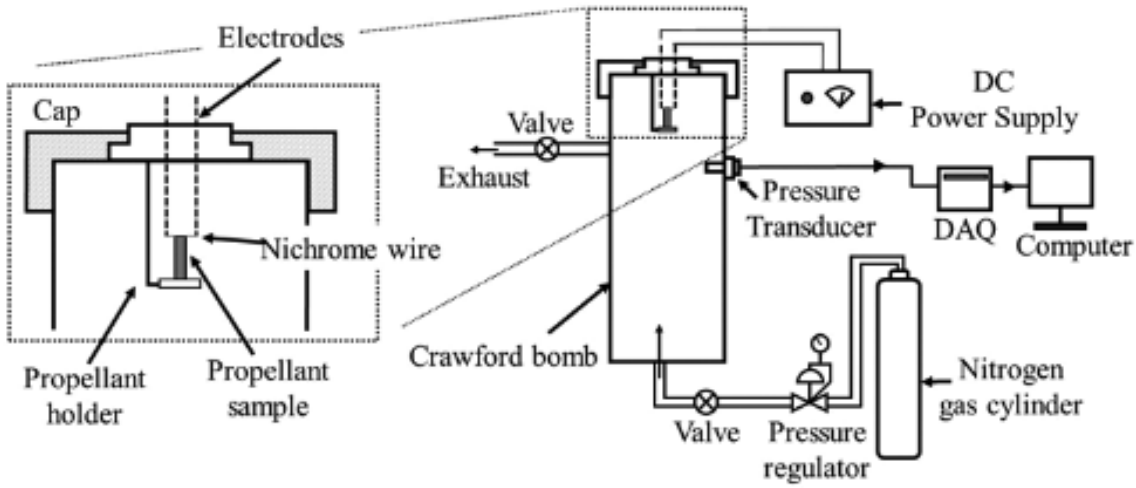

Figure 16: Schematic of the experimental setup to test the burn rates of the propellent[48]

2.3.11 Optimizing Propellant Composition

The researchers found the fuel-rich propellant with a composition of 35% ammonium perchlorate with 1% iron oxide embedded, 30% mechanically activated aluminum with 10% polytetrafluoroethylene (PTFE), and 25% HTPB was most suitable for this application [48]. This propellant provided the highest burn rates among all developed propellants with a high-pressure index of 0.58, making it suitable for ramjets requiring higher burn rates at lower possible primary

chamber pressures. The Young's modulus and tensile strength of this propellant were measured to be 1.73 MPa and 0.24 MPa, respectively [48].

2.3.12 Burn Rate and Pressure Index Observations

Burn rate tests conducted in a Crawford bomb showed that all five developed fuel-rich propellants had zero residues. Propellant F2 exhibited higher burn rates for pressures up to 60 bar than propellant F1 due to its higher Al loading [48]. However, there was a drop in the pressure index from 0.45 to 0.28, resulting in comparatively lower burn rates at higher pressures (above 60 bar). This reduction is consistent with previous findings by Verma and Ramakrishna [49], who reported that the value of n increases with a reduction in the particle size of Al.

Using mechanically activated Al by PTFE led to higher burn rates for propellants F3 and F4 compared to F1 and F2 at all pressures [48]. Around 60-75% higher burn rates were observed using PTFE and pyral in the propellants. Nevertheless, the pressure index decreased from 0.45 for propellant F1 to 0.35 and 0.4 for propellants F3 and F4, respectively [48]. This decrease is in line with the results obtained by Gaurav and Ramakrishna [50]. Furthermore, propellant F5 provided the highest burn rates among all the propellants, with a 68-86% increase in burn rates due to using both burn rate modifier IO embedded on AP and activated Al with PTFE [48]. According to Ishitha and Ramakrishna [51], the increase in n when AP was embedded with IO was likely due to the reduced binder melt associated with IO addition.

2.3.13 Gun-Launched Ramjet Propelled Artillery Shells

The increasing demand for extended-range artillery has led to exploring new propulsion technologies, such as gun-launched ramjet engines, for 155 mm howitzer systems. The adoption of solid fuel ramjet (SFRJ) engines in artillery projectiles can lead to a new generation of extended-range artillery, meeting the demands of modern military operations.

2.3.14 Design and Optimization for Extended Range

Kanga et al. investigated the design of a 155 mm gun-launched ramjet-propelled artillery shell using an inviscid flow assumption [38]. They focused on designing the projectile's air intake, combustion chamber, and nozzle while considering inviscid flow. Through a parameter study, they aimed to achieve a range of more than 80 km and maximize the high explosive volume [38].

2.3.15 Challenges and Solutions

Previous ramjet-propelled shells had allocated too much internal volume to the ramjet engine, resulting in reduced warhead volume and diminished effectiveness [38]. To address this issue, Kanga et al.'s study sought to propose a configuration that maximized the high explosive volume [38]. By varying design parameters, they aimed to achieve a range of more than 80 km [38].

2.3.16 Future Research

Future research in the area of solid fuel ramjet and solid fuel scramjet engines should focus on the following:

1. Development of advanced materials and fuel sources to enhance the performance and efficiency of these propulsion systems.
2. Optimize the shape and design of artillery projectiles and hypersonic vehicles to maximize their aerodynamic performance, range, and payload capacity.
3. Exploration of alternative propulsion systems, such as combined engines or hybrid systems, could provide additional efficiency, versatility, and adaptability advantages.
4. Investigation of these propulsion technologies' environmental and operational impacts, including their effects on air quality, noise pollution, and potential hazards to personnel and infrastructure.
5. Study the integration of these advanced propulsion systems into existing and future military and aerospace platforms and the development of appropriate support infrastructure and maintenance procedures.

By addressing these research areas, the development of solid-fuel ramjet and solid-fuel scramjet engines has the potential to revolutionize the field of propulsion systems, providing significant

advantages in terms of range, efficiency, and performance for artillery systems, hypersonic vehicles, and other aerospace applications.

2.3.27 Concluding Remarks

This literature review has provided an extensive overview of recent research and developments in solid fuel ramjet (SFRJ) and solid fuel scramjet (SFSJ) engine technologies. It has highlighted the potential of these advanced propulsion systems in revolutionizing the fields of artillery systems and hypersonic vehicles, offering significant advantages in terms of range, efficiency, and performance.

The review has discussed various aspects of SFRJ and SFSJ engine technologies, including designing and optimizing long-range artillery projectiles with rocket ramjets, the development of combined solid rocket/scramjet engines, and the utilization of solid fuel-rich propellants for ramjet applications. It has also explored the challenges associated with designing and optimizing gun-launched ramjet-propelled artillery shells and the ongoing research in this area.

Several key findings have emerged from the studies examined in this review. These findings include the potential for SFRJ engines to enhance the range and performance of artillery systems significantly, the advantages of combining solid rocket and scramjet propulsion systems for hypersonic vehicles, and the importance of optimizing fuel compositions and burn rates in solid fuel-rich propellants for ramjet applications.

Furthermore, the review has identified several critical areas for future research in solid-fuel ramjet and solid-fuel scramjet engine technologies. These areas include developing advanced materials and fuel sources, optimizing aerodynamic designs, exploring alternative propulsion and hybrid systems, and investigating these propulsion technologies' environmental and operational impacts.

In addition to these research directions, the integration of SFRJ and SFSJ engines into existing and future military and aerospace platforms will be essential for fully realizing the potential of these advanced propulsion systems. This will involve the development of appropriate support

infrastructure, maintenance procedures, and adapting existing systems to accommodate these new technologies.

In conclusion, solid-fuel ramjet and solid-fuel scramjet engines hold immense promise for revolutionizing the field of propulsion systems, with significant implications for the future of artillery systems, hypersonic vehicles, and other aerospace applications. Continued research and development efforts in this field are crucial for overcoming the challenges associated with these technologies and unlocking their full potential to transform military and aerospace capabilities.

2.4 Dynamic Equations of Motion

2.4.1 Introduction

Projectile motion is a fundamental area of study in classical mechanics, with applications spanning various fields such as sports, military technology, aerospace, and physics education. The study of projectile motion helps researchers and engineers understand the dynamics of objects propelled through the air and subject to gravitational and aerodynamic forces. Over the years, researchers have developed a range of simulation techniques and computational methods to predict and analyze projectile motion, including computational fluid dynamics (CFD), rigid body dynamics (RBD), and numerical modeling and spreadsheets in educational settings.

This literature review aims to provide a comprehensive overview of recent advancements and research in the field of projectile motion, focusing on three main areas: (1) the application of CFD and RBD methods in the analysis of projectile motion, (2) the study of aerodynamics in gun systems, and (3) the use of spreadsheets in teaching projectile motion. The first area covers studies that investigate the capabilities of accurately predicting projectiles' six-degrees-of-freedom (6DoF) trajectory and the aerodynamic analysis of projectiles during the gun system firing process. The second area discusses research that explores the impact of fabrication errors on the dynamic unbalance of howitzer projectiles and the effects of wind on projectile motion. The third area highlights the potential of using spreadsheet software such as Microsoft Excel in promoting STEM education among high school students, focusing on developing spreadsheet applications to simulate fall and projectile motion in the air.

By examining these studies and their findings, this review aims to thoroughly understand the current research in projectile motion and its various applications while identifying trends, gaps, and future directions for this critical study area.

2.4.2 The Use of Spreadsheets in Teaching Projectile Motion

The integration of technology in the classroom has the potential to enhance student learning and engagement. In particular, spreadsheet programs like Microsoft Excel have been explored as a tool for teaching various subjects, including physics, mathematics, and biology. Excel can be used to model real-world situations, enabling students to gain a deeper appreciation for the subject matter's applicability. This literature review examines several studies investigating the use of Excel in teaching STEM subjects and its potential to promote STEM education among high school students. The following passage discusses an experiment in which high school students developed spreadsheet applications to simulate fall and projectile motion in the air and its positive impact on their interest and motivation in STEM fields.

The use of spreadsheet programs, such as Microsoft Excel, has been explored as a tool for teaching various subjects, including physics, mathematics, and biology [52] [53] (Benacka, 2008; Benacka, 2013). In particular, Excel is an effective tool for introducing students to 3D graphics and enabling them to practice vector algebra [54] (Benacka, 2015a). Moreover, it has been used to simulate projectile motion in a vacuum [55](Benacka, 2015b) and to demonstrate the relationship between the elevation angle, points of shot, and impact of a projectile [53] (Benacka, 2015c). Excel has also been used to introduce integral calculus at the high school level by helping students calculate area and volume [52] (Benacka, 2015d).

Using numerical spreadsheet modeling in secondary school physics and biology has positively affected students' engagement and understanding of the subject [53] (Benacka, 2008). For example, students have been shown to benefit from using Excel in learning about projectile motion against an inclined plane [56](Benacka & Stubna, 2009) and in modeling animal populations at the high school level [57] [58](Benacka & Ceretkova, 2013, 2014). In addition, using spreadsheets to develop an understanding of science effectively engages students [59](Brosnan, 1994).

Integrating technology in teaching, including Excel, can improve student outcomes in mathematics and science [60](Crook, Sharma, & Wilson, 2015). Excel can provide a platform for students to engage in mathematical modeling, a valuable science education skill [65] (Keune & Henning, 2003). Furthermore, using Excel in conjunction with other subjects, such as physics, has fostered an interdisciplinary approach to learning [64] (Benacka, 2011).

Excel has proven to be a valuable tool in teaching various subjects, including physics, mathematics, and biology. Its use in the classroom can foster interdisciplinary learning and enhance student engagement and understanding of complex concepts. By using Excel to model real-world situations, students can gain a deeper appreciation for the applicability of the subject matter they are learning [61] [57] [58](Benacka, 2010, 2011; Benacka & Ceretkova, 2013, 2014). Another paper discusses an experiment in which 68 high school students aged 16-19 developed spreadsheet applications simulating fall and projectile motion in the air, applying the Euler method to solve governing differential equations [62]. The experiment aimed to promote STEM to these students and motivate them to pursue STEM fields in higher education. A questionnaire survey revealed that 97% of the students found the lessons interesting, and 85% wanted to continue modeling more complicated problems [63]. This finding aligns with the results of Benacka and Ceretkova (2014), suggesting that developing spreadsheet applications that model natural dynamic systems using the Euler method has the potential to promote STEM education among high school students [62]. Numerical modeling with spreadsheets can make lessons more engaging, benefit learning, and contribute to students' scientific and technological knowledge [62].

2.4.3 6DoF Trajectory Prediction and Flare-Stabilized Projectiles

Klatt, Proff, and Hruschka [64] conducted a study that aimed to investigate the capabilities of accurately predicting the six-degrees-of-freedom (6DoF) trajectory and the flight behavior of a flare-stabilized projectile using computational fluid dynamics (CFD) and rigid body dynamics (RBD) methods.

Klatt, Proff, and Hruschka (2019) conducted a study that aimed to investigate the capabilities of accurately predicting the six-degrees-of-freedom (6DoF) trajectory and the flight behavior of a flare-stabilized projectile using computational fluid dynamics (CFD) and rigid body dynamics

(RBD) methods. In their research, they compared two different approaches for calculating the trajectory. The first approach involved determining the projectile's wholly static and dynamic aerodynamic coefficients matrix using static and dynamic CFD methods. The second approach simulated the trajectories by solving the 6DoF motion equations directly coupled with time-resolved CFD methods. This discrete database and the data extracted from free-flight experiments were then used to simulate flight trajectories with an in-house developed 6DoF solver.

The findings of their study revealed that virtual fly-out simulations using RBD/CFD coupled simulation methods closely reproduced the motion behavior exhibited by the experimental free-flight data. However, using the discrete database of aerodynamic coefficients derived from CFD simulations resulted in slightly different flight behavior. The authors identified a discrepancy between the CFD 6DoF/RBD simulations and the results obtained by the MATLAB 6DoF-solver based on discrete CFD data matrices. They speculated that not all dynamic effects on the aerodynamics of the projectile were captured by the determination of the force and moment coefficients with CFD simulations based on the classical aerodynamic coefficient decomposition. This study contributes valuable insights into the limitations of current CFD methods and provides a foundation for further research on improving the prediction of projectile flight behavior.

2.4.4 Aerodynamic Analysis of Projectiles in Gun System Firing Process

Yu and Zhang [65] conducted an aerodynamic analysis of a projectile during the gun system firing process, focusing on the importance of the shot ejection process for shot accuracy.

Yu and Zhang (2010) conducted an aerodynamic analysis of a projectile during the gun system firing process, focusing on the importance of the shot ejection process for shot accuracy. The authors recognized that most research on muzzle flow has primarily concentrated on the blowout of high-pressure jet flow after the projectile exits the muzzle, often neglecting the interior ballistic process or the mutual influence between the moving projectile and muzzle flow. Yu and Zhang coupled the interior ballistic process with the flow simulation near the muzzle to address these limitations using a hybrid structured-unstructured gridding method.

The authors highlighted the complex and transient nature of the formation and development of the muzzle flow field. Their simulation results revealed that the projectile's muzzle velocity was 893.99 m/s, while its maximum velocity reached 899.28 m/s. The projectile velocity increased rapidly up to 0.8 ms after muzzle exit before gradually increasing to reach its maximum value. The maximum Mach number of the flowing gas increased to 6.83, and the breech pressure decreased to 21.5 MPa at 1.8 ms after the projectile exited the muzzle.

Yu and Zhang's findings, which demonstrated good agreement between the predicted muzzle velocity and maximum barrel pressure and those measured in gun firings, contribute to a deeper understanding of the aerodynamic process of gun system launching. Their research offers significant guidance for improving shot accuracy and muzzle brake design, addressing gaps in the existing literature by considering the mutual influence between the moving projectile and the muzzle flow during the gun firing process.

2.4.5 Aerodynamics of Gun Systems

Projectile dynamics is an important area of research with applications in both combat and sporting scenarios. In this literature review, we explore two studies that provide valuable insights into the behavior of projectiles. The first study by Chistyakov proposes a new method for integrating the equations of motion that consider wind effects. The second study by Zhang, Meng, and Wang investigates the impact of fabrication errors on the dynamic unbalance of howitzer projectiles. By examining these studies, we can better understand the dynamics of projectiles and improve their performance and safety in practical applications.

In the literature review, Chistyakov's work [63] presents a novel numerical method for integrating the dynamical equations of planar projectile motion, considering the effects of wind. The study addresses the shortcomings of traditional methods that rely on Cartesian coordinates and time by introducing a method based on Legendre transformation. This innovative approach reduces the number of functions from three to two, simplifying the problem while eliminating computational complexities and enhancing the accuracy of the results.

The author investigates the primary ranges of aerodynamic parameters at which different behaviors of the attack angle versus slope take place, including quasi-stabilization and aperiodic auto-oscillations. Additionally, the study reveals non-monotonous behavior of speed with two minima while the projectile descends if launched at angles close to 90°.

Chistyakov's method applies to a wide range of projectiles, such as arch arrows, lances, finned rockets, and others, demonstrating its potential for improving the performance of actual combat or sporting projectiles. With further development, this technique can be implemented into ballistic calculators, offering enhanced performance and increased reliability for users in the field. Furthermore, the method can be used in various practical applications, including exterior ballistics of sporting and combat projectiles, target engagement, and ease of use.

In the study of howitzer projectile dynamics, Zhang, Meng, and Wang [66] explored the effects of fabrication and assembly errors on the dynamic unbalance of the warhead and fuse in a 155 mm howitzer projectile. These imbalances can negatively impact the safety and reliability of the fuse. To determine the exterior ballistics motion of the projectile, the authors analyzed the six-dimensional rigid body motion equations and obtained the required aerodynamic parameters through simulation. Their research not only verified the credibility of the simulation method but also provided valuable insights into the safety and reliability of the fuse under dynamic, unbalance conditions.

2.4.6 Conclusion

This literature review has provided an in-depth analysis of recent advancements and research in the field of projectile motion, with a focus on simulation techniques, computational fluid dynamics, aerodynamics in gun systems, and the application of spreadsheet software such as Microsoft Excel in education. By examining the studies discussed in this review, we have gained valuable insights into the complexities and nuances of projectile motion and the various methods used to predict, analyze, and teach this fundamental aspect of classical mechanics.

In the realm of CFD and RBD methods, researchers have made significant strides in improving the accuracy of 6DoF trajectory predictions for flare-stabilized projectiles and the aerodynamic analysis of projectiles during the gun system firing process. These advancements contribute to our understanding of projectile motion and its behavior under various conditions, ultimately informing the design and optimization of projectiles and gun systems.

Furthermore, research in aerodynamics in gun systems has shed light on the effects of fabrication errors on the dynamic unbalance of howitzer projectiles and the impact of wind on projectile motion. These findings are crucial for enhancing projectiles' safety, reliability, and performance in real-world scenarios, paving the way for further advancements in the field.

Lastly, spreadsheet software, such as Microsoft Excel, teaching projectile motion has demonstrated promising potential in promoting STEM education among high school students. Educators can spark interest in STEM fields by engaging students in developing spreadsheet applications to simulate fall and projectile motion in the air and encourage students to pursue higher education in these disciplines.

In conclusion, the research surrounding projectile motion continues to grow and evolve, leading to discoveries, insights, and applications that expand our knowledge and inform future progress in this critical study area. As researchers and educators continue to push the boundaries of our understanding of projectile motion, it is anticipated that further advancements will emerge, shaping the future of this fascinating and important field.

3. Problem Formulation

3.1 Redesign of Geometry

In this chapter, we will focus on the crucial aspect of redesigning the geometry of the 155mm artillery shell to accommodate the integration of a ramjet engine. The primary motivation behind this redesign is to enhance the capabilities of the artillery shell by incorporating advanced propulsion technology, which will necessitate modifications to the current geometry.

The chapter will begin with a comprehensive examination of the existing geometry of the 155mm artillery shell. We will then present the proposed redesigned geometry, detailing the key changes made to facilitate the integration of the ramjet engine. The primary alterations to the geometry will include an increase in the overall length of the shell and the addition of rear fins to enhance stability at high speeds.

Finally, we will conclude this chapter by summarizing the main findings and contributions, emphasizing the importance of the proposed redesign in advancing artillery technology. This chapter aims to provide a solid foundation for understanding the geometric redesign and its significance in the context of ramjet-powered artillery shells.

3.1.1 Existing Geometry of the 155mm Artillery Shell

The 155mm artillery shell is a widely used caliber for artillery systems across the globe, known for its effectiveness and versatility in various military scenarios. The current geometry of the 155mm artillery shell has been developed and refined over several decades to optimize its performance in terms of range, accuracy, and stability. This section will discuss the key features of the 155mm artillery shell geometry, providing a foundation for understanding the proposed redesign.

3.1.2 Shell Components and Dimensions

Figure 17 155mm Legacy Shell

The existing geometry as shown in figure 17 above of the 155mm artillery shell consists of several essential components, including the nose cone, shell body, rotating band, and driving band. The nose cone is typically ogive-shaped to reduce aerodynamic drag and improve stability during flight. Depending on the mission requirements, the shell body houses the payload, which may consist of high explosives, submunitions, or other payloads. The rotating band encircles the shell body, allowing the shell to spin-stabilize during flight. In contrast, the driving band engages the rifling in the barrel, ensuring proper alignment and sealing during firing.

The dimensions of the 155mm artillery shell vary depending on the specific shell type and its intended application. However, a typical 155mm artillery shell has a diameter of 155mm and an overall length of approximately 698mm. The shell weight can range from 44kg depending on the specific shell type and payload.

3.1.3 Aerodynamics and Stability

The existing geometry of the 155mm artillery shell has been designed to optimize its aerodynamic performance and stability during flight. The ogive-shaped nose cone reduces drag, allowing the shell to maintain its velocity and trajectory more effectively than a blunt-nosed design.The smooth shell body further minimizes air resistance,while the rotating band imparts spin stabilization, which helps maintain the shell's orientation and stability during flight.

3.1.4 Limitations of the Existing Geometry

While the existing geometry of the 155mm artillery shell is highly effective in its intended role, some limitations may hinder the integration of advanced propulsion technologies like ramjet engines. The shell's aerodynamic properties may not be optimized for the high-speed flight regime that ramjet propulsion would enable. Specifically, the current geometry does not provide sufficient space to accommodate the ramjet engine.

In the following sections, we will discuss the proposed redesigned geometry of the 155mm artillery shell, which aims to address these limitations and facilitate the integration of the ramjet engine.

3.1.5 Redesigned Geometry of the 155mm Artillery Shell

A redesign is necessary to integrate the ramjet propulsion system and address the limitations of the existing 155mm artillery shell geometry. The proposed redesigned geometry aims to optimize the shell's range, accuracy, and stability at high speeds while providing the required space for the ramjet engine and its associated components. This section will discuss the key features and modifications of the redesigned 155mm artillery shell geometry.

3.1.6 Shell Components and Dimensions

The redesigned 155mm artillery shell retains many of the essential components of the existing geometry, such as the nose cone, shell body, rotating band, and driving band. However, several modifications have been made to accommodate the ramjet engine and improve the shell's performance at high speeds:

1. Increased Length: The overall length of the redesigned shell has been increased to provide additional space for the ramjet engine, its associated components, and fuel storage. The exact length after redesigning and integrating is 877mm.
2. Rear Fins: A set of rear fins has been added to the redesigned shell to improve stability during high-speed flight. These fins provide additional aerodynamic stability and control, ensuring the shell maintains its orientation and trajectory during high-speed maneuvers.

3. Ramjet Engine Integration: A 155mm ramjet engine has been integrated into the redesigned shell geometry. The engine is positioned towards the center of the shell to maintain the center of gravity and minimize the impact on the shell's aerodynamic properties. The ramjet engine inlet is located at the cone of the shell, allowing for efficient air intake during flight.

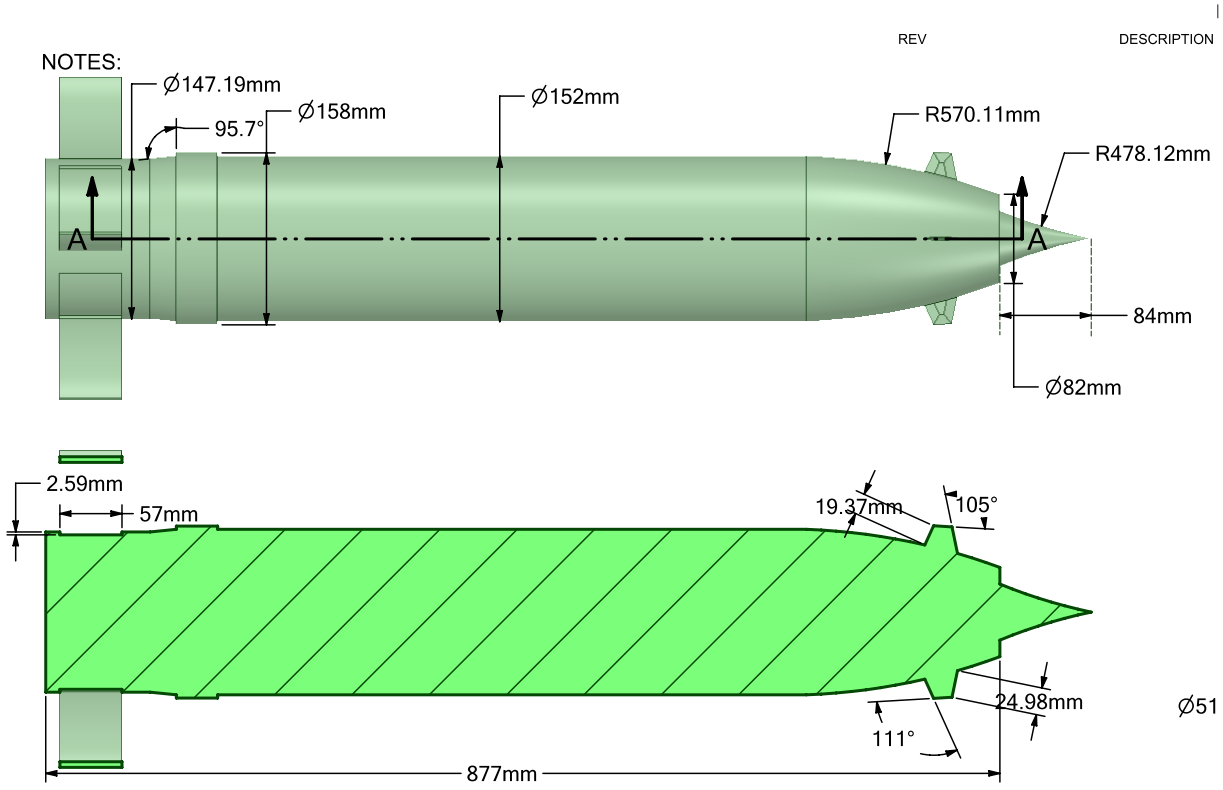

Figure 18 Redesigned 155mm Ramjet Powered Artillery Shell

3.1.8 Aerodynamics and Stability

The redesigned geometry of the 155mm artillery shell has been optimized for aerodynamic performance and stability at high speeds. The increased length, rear fins, and ramjet engine integration contribute to the shell's improved aerodynamic properties, ensuring efficient flight characteristics and stability during high-speed operations. The shell's spin stabilization, provided by the rotating band, is maintained in the redesigned geometry, further enhancing the shell's stability during flight.

3.1.9 Advantages of the Redesigned Geometry

The proposed redesigned geometry of the 155mm artillery shell offers several advantages over the existing geometry, including:

1. Increased Range: The integration of the ramjet engine allows the redesigned shell to achieve significantly greater range compared to conventional artillery shells, potentially doubling or even tripling the effective range.
2. Improved Accuracy: The increased aerodynamic stability and control provided by the rear fins and optimized geometry contribute to improved accuracy during high-speed flight, enabling the shell to engage targets more effectively at extended ranges.
3. Enhanced Versatility: The redesigned geometry, combined with the ramjet propulsion system, offers the potential for enhanced versatility regarding mission capabilities, including rapid response and deep-strike operations.

In conclusion, the 155mm artillery shell's redesigned geometry seeks to address the existing geometry's limitations and facilitate the integration of the ramjet propulsion system, offering a promising solution for enhancing the performance and capabilities of artillery systems.

3.2 Aerodynamic Validation Via Missile DATCOM

3.2.1 Introduction

This chapter presents the aerodynamic validation of the redesigned artillery shell using Missile DATCOM, a widely used software tool for preliminary aerodynamic analysis of missile and rocket configurations. The focus will be on comparing the aerodynamic performance of the existing artillery shell with the redesigned shell, which features an increased length, the addition of rear fins for improved stability at high speeds, and the integration of a 155mm ramjet engine.

3.2.2 Missile DATCOM Methodology

Missile DATCOM uses a component-buildup approach to estimate aerodynamic coefficients for the entire configuration. The methodology involves dividing the geometry into smaller

components, estimating the coefficients for each component, and then summing the contributions to obtain the total coefficients.

3.2.3 Existing Artillery Shell Geometry

The existing artillery shell has the following geometry and firing conditions:

- Caliber: D = 155 mm
- Overall Length: Lt = 698 mm
- Total Mass: Mt = 43 kg
- Center of Gravity from the Nose Tip: C.G_x = 0.459 m
- Axial Moment of Inertia: I_xx = 0.144 kg.m2
- Lateral Moment of Inertia: I_yy = I_zz = 1.216 kg.m2
- Shell muzzle velocity: Vo = 684.3 m/s
- Shell muzzle spin rate: po = 175.48 rps
- Firing Elevation Angle: θ = 44°

Redesigned Artillery Shell Geometry

The redesigned artillery shell features the following geometry and firing conditions:

- Caliber: D = 155 mm
- Overall Length: Lt = 877 mm
- Total Mass: Mt = 54.2 kg
- Center of Gravity from the Nose Tip: C.G_x = 0.4805 m
- Axial Moment of Inertia: I_xx = 0.144 kg.m2
- Lateral Moment of Inertia: I_yy = I_zz = 1.216 kg.m2
- Shell muzzle velocity: Vo = 684.3 m/s
- Shell muzzle spin rate: po = 175.48 rps
- Lref: 0.961 m
- Sref: 0.018136 m2
- Rear Fins Data: Ctp = 0.057, Crt = 0.057, t/c_tp = 0.003, t/c_rt = 0.003
- Firing Elevation Angle: θ = 44°

3.2.4 Aerodynamic Coefficient Analysis

Tabulated below are the Coefficients of Drag, Lift & Moment, Respectively, from Missile DATCOM based on the input data mentioned in Section 3.2.3.

Table 2 Drag Coefficients

C_D (Mach/Alpha)	-6	-4	-2	0	2	4	6
0.6	0.272	0.247	0.233	0.229	0.233	0.247	0.272
0.8	0.279	0.253	0.238	0.234	0.238	0.253	0.279
0.9	0.333	0.298	0.277	0.27	0.277	0.298	0.333
0.95	0.388	0.352	0.33	0.323	0.33	0.352	0.388
1	0.456	0.416	0.392	0.384	0.392	0.416	0.456
1.05	0.528	0.481	0.453	0.444	0.453	0.481	0.528
1.1	0.552	0.505	0.477	0.468	0.477	0.505	0.552
1.2	0.573	0.529	0.503	0.494	0.503	0.529	0.573
1.35	0.583	0.558	0.542	0.536	0.542	0.558	0.583
1.5	0.54	0.517	0.501	0.496	0.501	0.517	0.54
1.75	0.483	0.46	0.445	0.44	0.445	0.46	0.483
2	0.431	0.408	0.394	0.389	0.394	0.408	0.431
2.5	0.403	0.378	0.364	0.359	0.364	0.378	0.403
3.01	0.38	0.355	0.341	0.336	0.341	0.355	0.38
4.01	0.349	0.319	0.304	0.299	0.304	0.319	0.349
5.01	0.331	0.299	0.285	0.28	0.285	0.299	0.331
6.01	0.316	0.285	0.27	0.265	0.27	0.285	0.316

Table 3 Lift Coefficients

C_L (Mach/Alpha)	-6.000	-4.000	-2.000	0.000	2.000	4.000	6.000
0.6	-0.592	-0.392	-0.188	0.000	0.188	0.392	0.592
0.8	-0.613	-0.410	-0.199	0.000	0.199	0.410	0.613
0.9	-0.633	-0.425	-0.207	0.000	0.207	0.425	0.633
0.95	-0.649	-0.435	-0.211	0.000	0.211	0.435	0.649
1	-0.683	-0.458	-0.222	0.000	0.222	0.458	0.683
1.05	-0.794	-0.532	-0.259	0.000	0.259	0.532	0.794
1.1	-0.804	-0.539	-0.262	0.000	0.262	0.539	0.804
1.2	-0.747	-0.501	-0.244	0.000	0.244	0.501	0.747
1.35	-0.517	-0.358	-0.174	0.000	0.174	0.358	0.517
1.5	-0.476	-0.330	-0.162	0.000	0.162	0.330	0.476
1.75	-0.440	-0.301	-0.151	0.000	0.151	0.301	0.440
2	-0.420	-0.279	-0.143	0.000	0.143	0.279	0.420
2.5	-0.410	-0.271	-0.138	0.000	0.138	0.271	0.410
3.01	-0.403	-0.264	-0.134	0.000	0.134	0.264	0.403
4.01	-0.438	-0.251	-0.123	0.000	0.123	0.251	0.438
5.01	-0.441	-0.238	-0.115	0.000	0.115	0.238	0.441
6.01	-0.430	-0.249	-0.109	0.000	0.109	0.249	0.430

Table 4 Moment coefficients

Cm (Mach/ Alpha)	-6	-4	-2	0	2	4	6
0.60	0.163	0.110	0.053	0.000	-0.053	-0.110	-0.163
0.80	0.178	0.121	0.059	0.000	-0.059	-0.121	-0.178
0.90	0.191	0.129	0.063	0.000	-0.063	-0.129	-0.191
0.95	0.197	0.133	0.065	0.000	-0.065	-0.133	-0.197
1.00	0.208	0.140	0.068	0.000	-0.068	-0.140	-0.208
1.05	0.269	0.181	0.088	0.000	-0.088	-0.181	-0.269
1.10	0.268	0.180	0.088	0.000	-0.088	-0.180	-0.268
1.20	0.226	0.152	0.074	0.000	-0.074	-0.152	-0.226
1.35	0.127	0.086	0.041	0.000	-0.041	-0.086	-0.127
1.50	0.093	0.063	0.031	0.000	-0.031	-0.063	-0.093
1.75	0.066	0.046	0.023	0.000	-0.023	-0.046	-0.066
2.00	0.056	0.037	0.019	0.000	-0.019	-0.037	-0.056
2.50	0.039	0.026	0.013	0.000	-0.013	-0.026	-0.039
3.01	0.033	0.021	0.011	0.000	-0.011	-0.021	-0.033
4.01	0.027	0.012	0.006	0.000	-0.006	-0.012	-0.027
5.01	0.024	0.008	0.003	0.000	-0.003	-0.008	-0.024
6.01	0.020	0.008	0.001	0.000	-0.001	-0.008	-0.020

Using the provided drag, lift, and moment coefficient data from Missile DATCOM, the aerodynamic performance of the redesigned artillery shell is analyzed and compared to the existing shell. The analysis includes the evaluation of the drag polar, lift curve, and moment curve for the different Mach numbers and angles of attack in the figures below

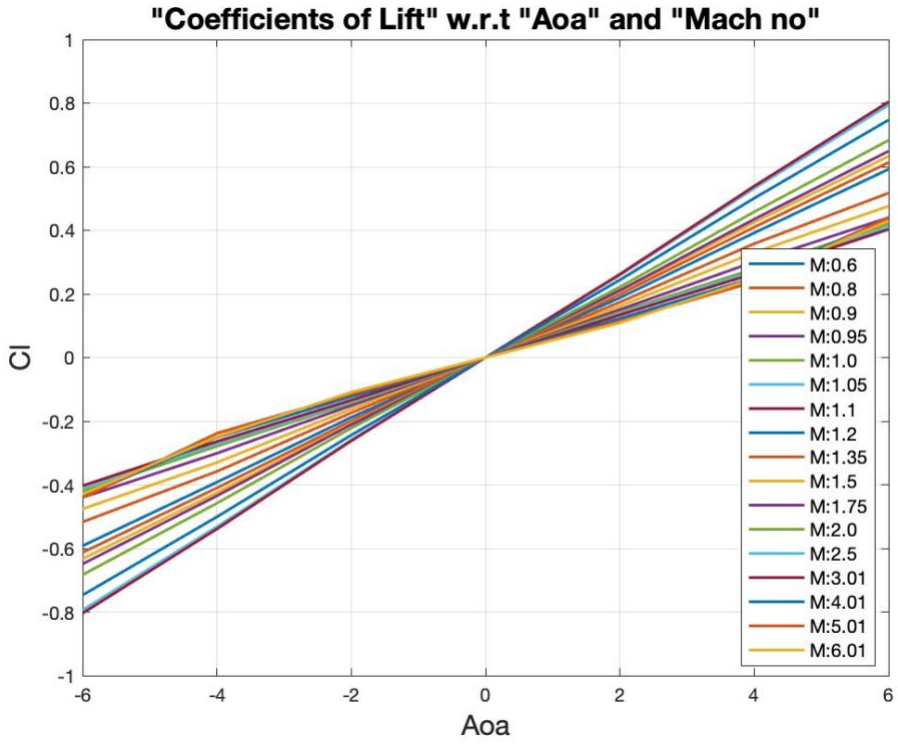

Figure 19 Coefficient of Lift wrt to AOA & Mach No

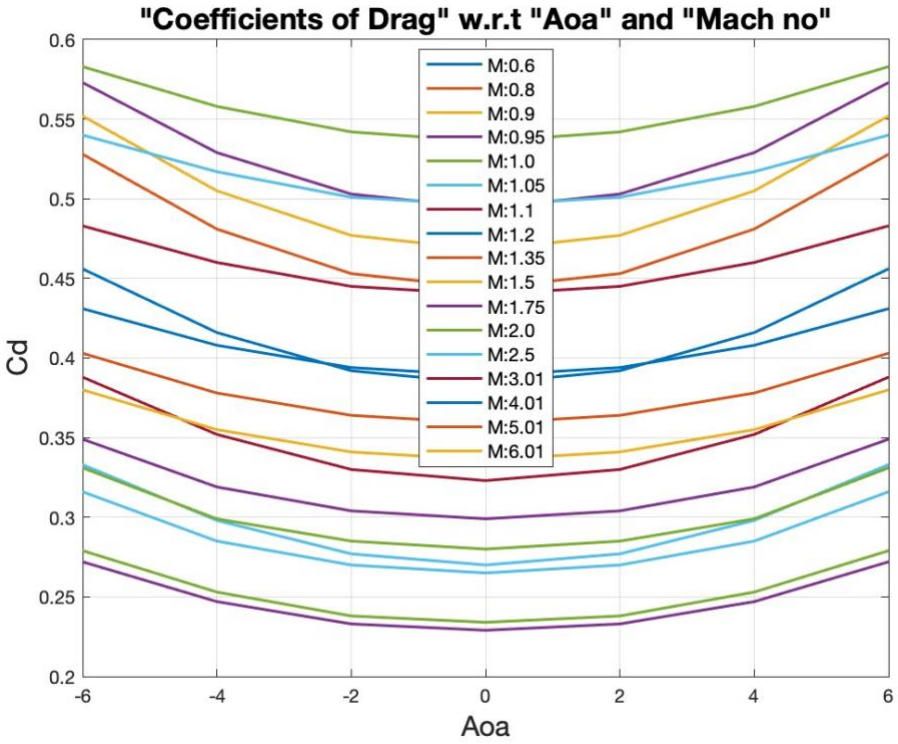

Figure 20 Coefficient of Drag wrt to AOA & Mach No

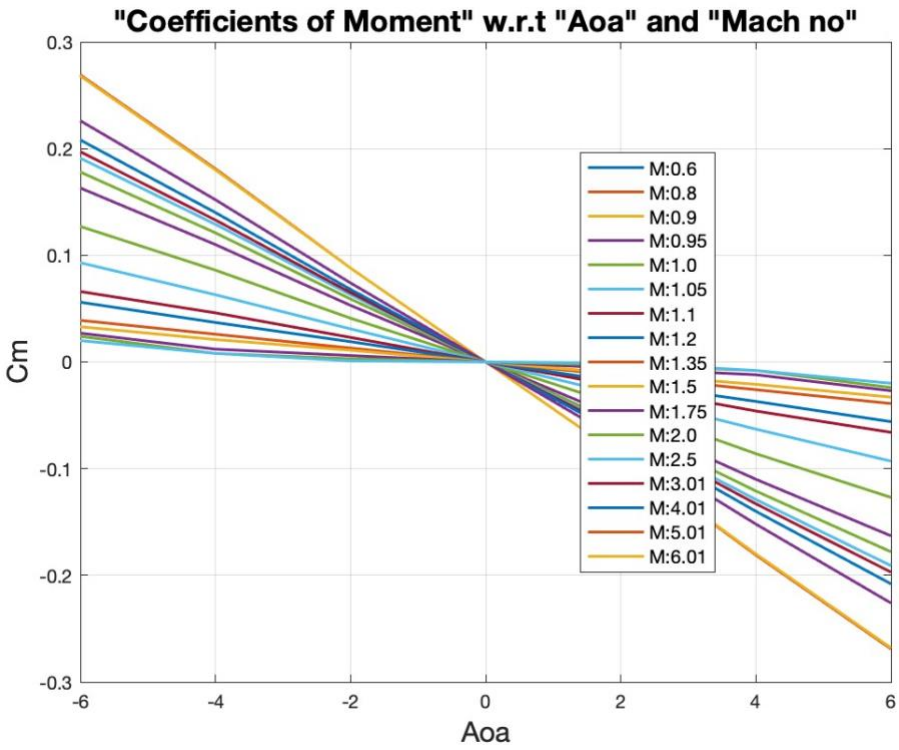

Figure 21 Coefficient of Moment wrt to AOA & Mach No

The drag coefficient data shows that the redesigned shell has a similar drag behavior across the range of Mach numbers and angles of attack compared to the existing shell. This indicates that the increase in length and addition of rear fins has not significantly affected the drag performance of the shell.

The lift coefficient data reveals that the redesigned shell exhibits higher lift coefficients at higher angles of attack than the existing shell. This can be attributed to the addition of rear fins, which improve the stability and lift performance at high speeds.

The moment coefficient data demonstrates that the redesigned shell has a similar moment behavior to the existing shell. This indicates that the changes in geometry have not significantly affected the stability of the shell in terms of its pitching moment.

3.2.5 Concluding Remarks

The aerodynamic validation results for the redesigned artillery shell using Missile DATCOM show that the redesigned shell maintains similar drag and moment performance compared to the existing shell while achieving improved lift performance at high angles of attack. This can be attributed to the increased length and the addition of rear fins, which enhance the stability and lift characteristics of the shell at high speeds. Consequently, the redesigned artillery shell is expected to offer superior aerodynamic performance, which could lead to improved range and accuracy in the field.

3.2.7 Future Work

Further studies and refinements can be carried out to optimize the aerodynamic performance of the redesigned artillery shell. These could include:

- Conducting wind tunnel tests to validate and refine the aerodynamic coefficients obtained from Missile DATCOM.
- Exploring the effects of varying fin geometry and size on the aerodynamic performance and stability of the shell.
- Investigating the impact of different nose shapes on drag reduction and overall performance.
- Performing a more detailed analysis of the interaction between the ramjet engine and the aerodynamics of the redesigned shell.

In conclusion, the aerodynamic validation of the redesigned artillery shell using Missile DATCOM has shown promising results, indicating potential improvements in range and accuracy. Further work in refining and optimizing the design could lead to even more significant performance enhancements, benefiting future artillery systems.

3.3 Design of 155mm Ramjet Engine

3.3.1 Introduction

Ramjet engines are air-breathing jet engines that operate by subsonic fuel combustion in a stream of air compressed by the aircraft's forward speed, as shown in Figure 22 below [67]. Due to their simplicity and lack of moving parts, ramjet engines are an attractive option for high-speed propulsion systems in applications such as missiles, hypersonic vehicles, and space launch systems [68]. This chapter aims to provide an in-depth discussion of the design process for a ramjet engine, including the essential components and performance parameters.

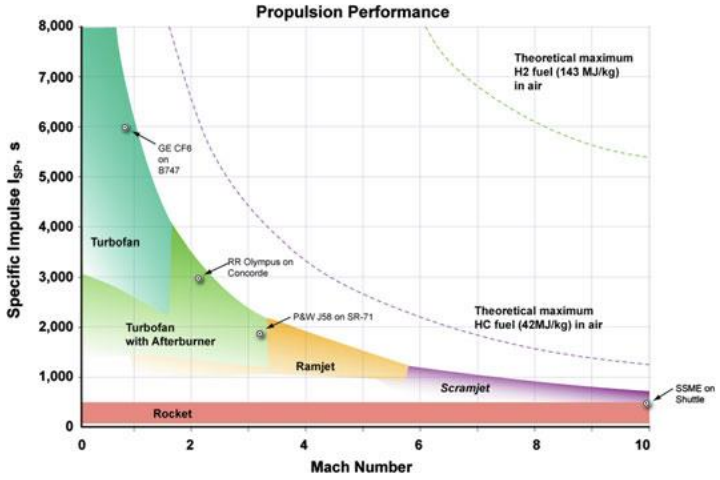

Figure 22 Characteristics Performance of Propulsion

3.3.2 Thermodynamic Cycle

Ramjet engines operate based on the Brayton cycle, which consists of four processes: adiabatic compression, constant pressure heat addition, adiabatic expansion, and constant pressure heat rejection [68]. In a ramjet engine, adiabatic compression occurs in the inlet, where the incoming air is decelerated and compressed due to the engine's forward motion. The constant pressure heat addition occurs in the combustion chamber, where fuel is injected, mixed with the compressed air, and burned [67]. The high-temperature combustion products then undergo adiabatic expansion in the nozzle, producing thrust as they accelerate to supersonic speeds.

3.3.3 Main Components

A ramjet engine consists of three primary components: the inlet, the combustion chamber, and the nozzle, as shown in Figure 23 below. The inlet captures and compresses the incoming air, slowing it down to subsonic speeds while increasing its pressure and temperature. The combustion chamber is where fuel is injected, mixed with compressed air, and ignited to release energy [69]. The combustion process increases the temperature and pressure of the gas, which then expands and accelerates through the nozzle to generate thrust [70].

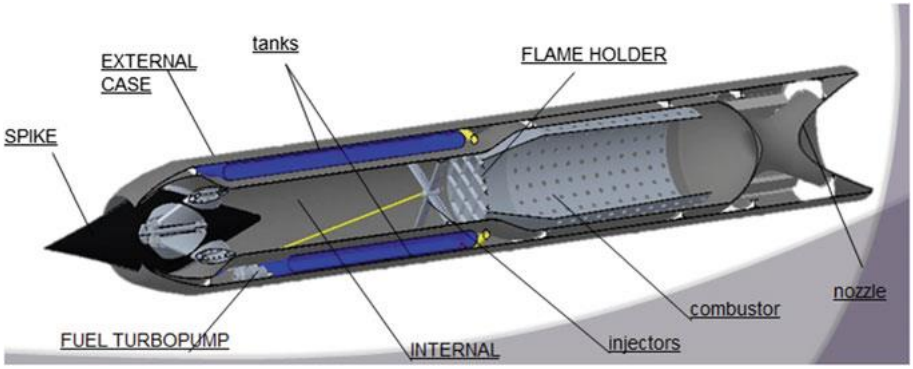

Figure 23 Components of Ramjet Artillery

3.3.4 Performance Parameters

The performance of a ramjet engine is characterized by several key parameters, including thrust, specific impulse, and efficiency [68]. Thrust is the force produced by the engine and is directly related to the mass flow rate of air and the velocity change of the exhaust gases. Specific impulse measures the engine's propulsive efficiency, defined as the thrust produced per unit mass flow rate of fuel consumed [69]. The efficiency of a ramjet engine can be expressed in terms of thermal efficiency (the ratio of useful work output to the heat input) and propulsive efficiency as shown in figure 25 below (the ratio of useful work output to the kinetic energy of the exhaust gases) [67]. Given the Atmospheric data as per the design calculations in the equations below, the temperature and pressure are Maximizing these efficiency values is essential for designing a high-performance ramjet engine.

Equation of Thrust:

$$F\ (H, M, q) = [mv\ .(1+q).W(H, M, q)] - mv.M.\sqrt{\kappa.R.Ta(H)} + A.(p9(H, M, q) - Pa(H))$$

Equation 1: Equation of Thrust

where:

- $F\ (H, M, q)$ is the function of Altitude, Macho No and Air to fuel ratio
- mv is mass flow rate
- $W\ (H, M, q)$is the exit velocity at a specific Altitude, Mach no and Air to fuel ratio
- $M\ is\ Mach\ No$
- q is Equivalence ratio of throttle
- κ is gamma constant which = 1.4
- R is gas constant = 287
- $Ta(H)$ is ambient temperature at a specific altitude
- A is exit nozzle area
- $p9(H, M, q)$ is static pressure at nozzle exit
- $Pa(H)$ is ambient pressure at a specific altitude

Equation of Specific Thrust:

$$Fsp(H, M, q) = \frac{F(H, M, q)}{mv}$$

Equation 2: Equation of Specific Thrust

where:

- $Fsp\ (H, M, q)$ is the specific thrust at a specific Altitude, Macho No and Air to fuel ratio
- $F\ (H, M, q)$ is the function of Altitude, Macho No and Air to fuel ratio
- mv is mass flow rate

Fuel Flow Rate:

$$mf = mv.A_p.qcp + mv.A_s.qcs + mv.A_{pilot}.qp$$

Equation 3: Equation of Fuel flow Rate

where:

- mf is the fuel flow rate
- mv is mass flow rate
- $A_p.qcp$ is the primary combustor area and fuel to air ratio of primary combustor
- $A_s.qcs$ is the secondary combustor area and fuel to air ratio of secondary combustor
- $A_{pilot}.qp$ is the pilot area and fuel to air ratio of pilot combustor

Specific Fuel Consumption:

$$Csp\ (H, M, q) = \frac{q.36000}{Fsp(H, M, q)}$$

Equation 4: Equation of Specific Fuel Consumption

where:

- $Csp\ (H, M, q)$ is the specific fuel consumption at a specific Altitude, Mach no and Air to fuel ratio
- q is Equivalence ratio of throttle
- $Fsp\ (H, M, q)$ is the specific thrust at a specific Altitude, Macho No and Air to fuel ratio

3.3.5 Design Objectives

The primary design objectives for the ramjet engine include a system diameter of 155 mm, a fuel mass of 5 kg, and a total system weight not exceeding 54 kg. The engine must utilize liquid kerosene as fuel and produce a thrust up to 2100 N, significantly increasing the projectile range. The engine starting condition is set at Mach 1.8.

3.3.6 Design Approach

A computational approach is adopted for the design process, leveraging mathematical models and software tools to optimize engine performance.

3.3.7 Tools and Methods

The ramjet engine is designed using MathCAD software, which enables the analysis and simulation of engine performance based on mathematical models.

3.3.8 Design Iteration

Given that the thrust profile in a ramjet engine is not constant, an iterative approach is employed to calculate thrust at 5-second intervals until the total 5 kg of fuel is consumed. Subsequently, the maximum range is calculated based on the thrust values. This iterative process allows for adjustments and refinements to the engine design, ensuring that the desired performance parameters are met.

3.3.9 Validation

The validation of the ramjet engine design is primarily based on a comparison with published data from existing ramjet engines. It is important to note that this mathematical design serves as a starting point and can be further optimized through physical prototyping.

3.4 Inlet Design

3.4.1 Inlet Types

a. Subsonic inlets: Designed for flight at subsonic speeds (Mach < 1), these inlets typically feature simple geometries, such as rectangular or circular shapes, with smooth, curved surfaces to guide the incoming air into the engine [68]. Subsonic inlets generally have lower pressure recovery and total pressure losses than supersonic inlets.

b. Supersonic inlets: For supersonic flight regimes (1 < Mach < 5), these inlets use a series of oblique shock waves to slow down and compress the incoming air to subsonic speeds before it enters the combustion chamber. Common supersonic inlet designs include the fixed-geometry inlet (e.g., Busemann inlet) and the variable-geometry inlet (e.g., two-dimensional, axisymmetric inlets with adjustable geometries to maintain optimal performance across a range of flight conditions) [71].

c. Hypersonic inlets: For flight speeds in the hypersonic regime (Mach > 5), these inlets are designed to minimize total pressure losses while maintaining efficient compression and deceleration of the airflow. Hypersonic inlets often employ mixed or pre-compression concepts, combining external and internal compression using shock waves and boundary layer interactions [72]

In the proposed design, the inlet chosen for this ramjet engine is a supersonic, external, three-dimensional (3D) type. This type of inlet is designed to handle the high-speed airflow entering the engine, efficiently compressing and slowing down the flow before it enters the combustion chamber. of design Mach 3.2 and above as per the design calculations in the equations below:

3.4.2 Inlet Geometry

The inlet geometry comprises a 30° cone with an intake capture area of 0.01 m². The inlet cone diameter is 135 mm, with a radius of 0.0564 m. The shock angle, which is the angle between the cone's surface and the incoming flow, is 37.79°. This geometry has been chosen to optimize the compression and deceleration of the incoming airflow, ensuring efficient performance under the engine's operating conditions.

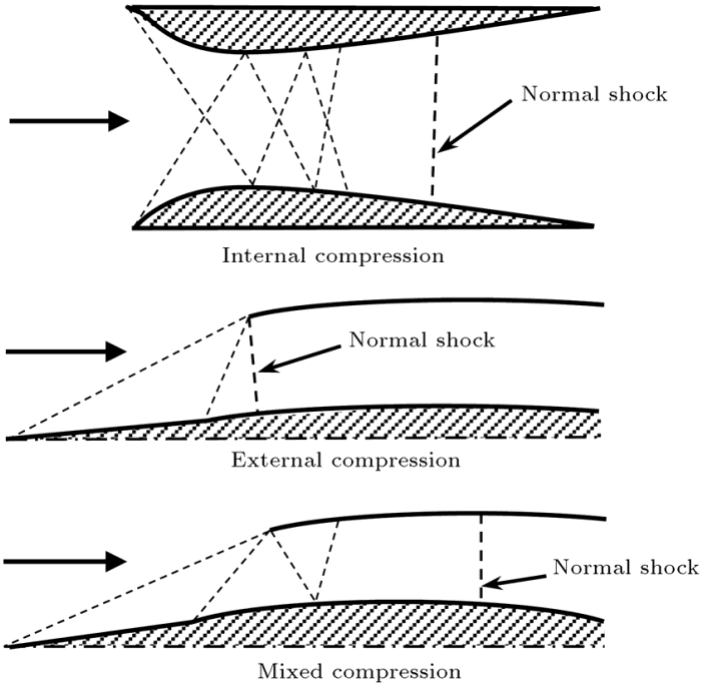

Figure 24 Types of Compressions in Normal Shock

3.4.3 Inlet Performance Parameters

The key performance parameters for the inlet are as follows: pressure recovery at the grid is 0.99 bar, total pressure loss is 5.63 x 10^5 Pa, and mass flow rate is 5.2 kg/s. These values are essential for evaluating the overall performance of the inlet design and its impact on the ramjet engine's efficiency.

3.4.4 Inlet Design Considerations

The engine's starting condition is Mach 1.8. After the first shock wave as per the design calculation in the equations below, the total pressure is 5.65 x 10^5 Pa, the Mach number is 1.6, and the Mach number at the cone surface is 1.4. The mid-value Mach number is 1.48, and the average Mach number is 1.47. The pressure recovery after the normal shock wave is 0.937 and the Mach No after the normal shock wave is 0.7095. These parameters have been considered in the design of the inlet to ensure proper operation and efficient performance under the engine's starting conditions and throughout its operational range.

Equations of Pressure Recovery after normal shock wave:

$$\sigma uN = \left[\frac{(1+\kappa)M1k^2}{(\kappa-1)M1k^2+2}\right]^{\frac{\kappa}{\kappa-1}} \cdot \left[\frac{(1+\kappa)}{2\kappa M1k^2-(\kappa-1)}\right]^{\frac{1}{\kappa-1}}$$

Equation 5: Equation of Pressure Recovery after first normal shock wave

where:

- σuN is the pressure recovery after normal shock recovery
- κ is gamma constant which = 1.4
- $M\ is\ Mach\ No$

Equations of Mach No after the normal shock wave:

$$M2 = \frac{(\kappa-1).M1k^2+2}{2.\kappa.M1k^2-(\kappa-1)}$$

Equation 6: Equation of Mach No after the normal shock wave

where:

- κ is gamma constant which = 1.4
- $M2\ is\ Mach\ No\ after\ normal\ shock\ wave$

Critical and Actual intake capture area ratio:

$$p \circ (H,M) = \frac{P0(H,M)}{(1+\frac{\kappa-1}{2}.M^2)^{\frac{\kappa}{\kappa-1}}} \qquad \psi(M) = \frac{M}{(1+\frac{\kappa-1}{2}.M^2)^{\frac{\kappa+1}{2.(\kappa-1)}}}$$

Equation 7: Equations of Critical and Actual Intake Capture Area Ratio

Where for equation 7 and 8:

- $p \circ (H,M)$ is the total pressure stagnation at a specific Altitude and Mach no
- $\psi(M)$ is the specific impulse as a function of Mach no

- $M\ is\ Mach\ No$
- κ is gamma constant which = 1.4

3.5 Combustion Chamber Design

3.5.1 Types of Combustion Chambers

a. Subsonic combustion chambers: Designed for combustion at subsonic speeds, these chambers typically feature relatively long and narrow geometries to ensure sufficient residence time for the combustion process [67]. In subsonic combustion chambers, the fuel-air mixture is well-mixed and burned nearly homogeneously, resulting in a stable flame front and lower peak temperatures [69].

b. Supersonic combustion chambers: Also known as scramjets, enable combustion at supersonic speeds. They have short and wide geometries to minimize pressure losses and maintain high-speed airflow through the chamber [73]. Fuel injection and mixing occur at supersonic velocities, resulting in a more distributed combustion process and higher peak temperatures than in subsonic combustion chambers [74].

c. Annular combustion chambers: These chambers feature a ring-shaped geometry surrounding the engine's central axis. They provide advantages in compactness, uniform temperature distribution, and lower pressure losses compared to traditional cylindrical combustion chambers [73] . Depending on the application, annular combustion chambers can be designed for subsonic or supersonic combustion.

3.5.2 Type of Combustion Chamber in Proposed Design

The combustion chamber for the 155mm ramjet-powered artillery shell is designed to facilitate efficient mixing and combustion of the fuel and air while meeting the operational requirements of the system. The overall length of the combustion chamber is 135 mm. The combustor features an annular grid-type design, which helps to maintain a uniform flow and temperature distribution within the chamber

3.5.3 Flame Stabilization and Injection Method

Flame stabilization within the combustion chamber is achieved using a pilot flame stabilizer. The pilot stabilizer operates at a temperature of 1.77×10^3 K, ensuring reliable ignition and stable combustion throughout the engine's operation. The fuel injection method employed in this combustion chamber is a kerosene spray, providing an efficient fuel-air mixture for combustion.

3.5.4 Combustor Inlet and Operating Conditions

The combustion chamber is designed to operate with a Mach number of 1.2 at the inlet, with an inlet pressure of 4.5 bar. The combustor efficiency is calculated to be 0.7255 as shown in figure 25, while the combustion stability is 0.0407. The combustion pressure loss within the chamber is 12%, which is an acceptable value for this type of application.

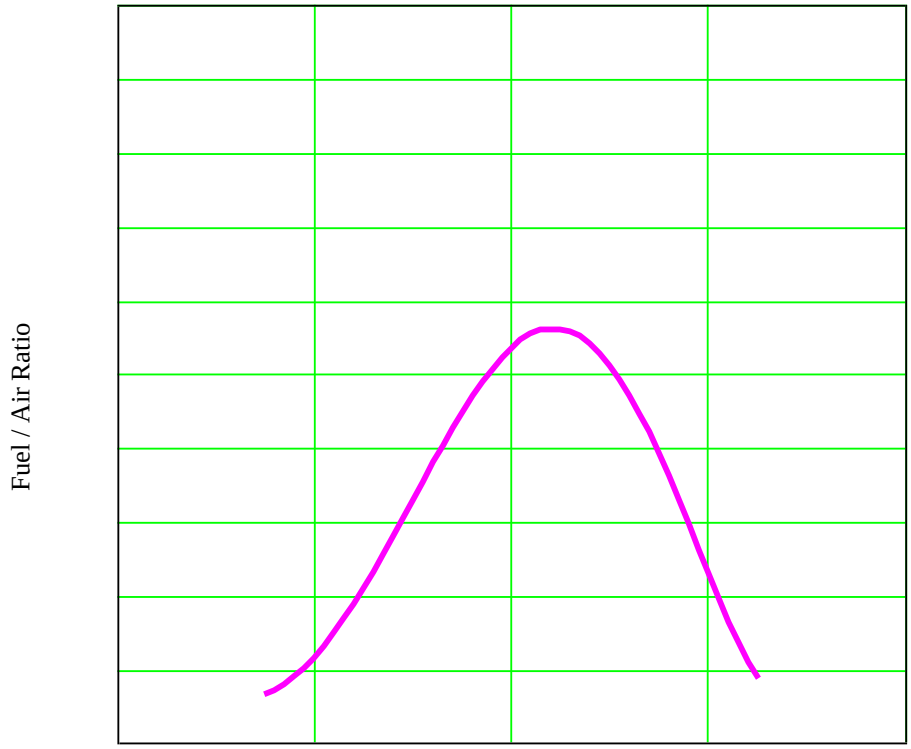

Figure 25 Combustor Efficiency Graph

3.5.5 Combustor Outlet and Performance

The combustion chamber operates at a temperature of 473 K and has an exit Mach number of 0.61. These conditions ensure the ramjet engine can achieve the desired thrust and performance throughout its operational envelope.

$$\sigma pg = \frac{1}{[1 + \frac{\kappa - 1}{2}.M6(H,M)^2.(1 - \frac{T6(H,M)}{T7(H,M,q)})]^{\frac{\kappa}{\kappa-1}}}$$

Equation 8:Equation for total pressure loss due to heat

$$\psi g(M) = \frac{M}{(1 + \frac{\kappa g - 1}{2}.M^2)^{\frac{\kappa g+1}{2.(\kappa g-1)}}}$$

Equation 9: Equation for total pressure after combustor

Where for equation 10 and 11:

- $\psi g(M)$ represents the specific impulse with respect to gravity as a function of Mach number (M)
- $M6\ is\ the\ Mach\ No\ at\ combustor\ inlet\ as\ a\ function\ of\ Altitude\ and\ Mach\ no$
- κ is gamma constant which = 1.4
- $T6(H,M)\ is\ the\ temperature\ at\ Grid\ a\ function\ of\ Altitude\ and\ Mach\ no$
- $T7(H,M,q) is\ the\ temperature\ at\ combustor\ exits\ a\ function\ of\ Altitude, Mach\ no\ and\ Air\ to\ fuel\ ratio$

In summary, the combustion chamber of the 155mm ramjet-powered artillery shell features an annular grid-type design with a pilot flame stabilizer and kerosene spray fuel injection. The chamber has been designed to operate efficiently under the specified conditions, with an inlet Mach number of 1.2, an inlet pressure of 4.5 bar, and a combustion temperature of 473 K. The combustion chamber's performance, including its efficiency, stability, and pressure loss, meets the requirements for this application as per the design calculations in the equations above.

3.6 Nozzle Design

3.6.1 Types of Nozzles

a. Converging nozzles: These nozzles are used for subsonic exhaust velocities and feature a decreasing cross-sectional area from the inlet to the outlet [67]. The converging shape accelerates the exhaust gases to generate thrust. However, these nozzles are not suitable for applications requiring supersonic exhaust velocities [69].

b. Converging-diverging nozzles: Also known as de Laval nozzles, these nozzles are designed for supersonic exhaust velocities. They consist of a converging section, a throat area, and a diverging section [67]. The nozzle accelerates the flow to supersonic speeds by first compressing it in the converging section, reaching sonic speed at the throat, and then expanding it in the diverging section, further accelerating the flow supersonic speeds [69].

c. Aerospike nozzles: These nozzles employ a central spike that extends aft of the engine, with the exhaust gases flowing around the spike's outer surface .The aerospike nozzle can self-adapt to varying altitude and flight conditions, providing efficient expansion and high thrust across various operating conditions.This nozzle design suits application requiring high altitude or variable flight regimes.

3.6.2 Type of Nozzle in Proposed Design

The nozzle chosen for the 155mm ramjet-powered artillery shell is convergent-divergent. This type of nozzle is designed to accelerate the flow from subsonic to supersonic speeds, which is essential for maximizing the performance of the ramjet engine. The convergent-divergent nozzle features a throat diameter of 123 mm, the narrowest part of the nozzle, where the flow reaches its highest velocity before expanding in the divergent section.

3.6.3 Nozzle Performance and Conditions

The nozzle is designed to achieve an exit velocity of 824.5 m/s as per the equation below, which is critical for providing the necessary thrust to propel the artillery shell. The nozzle's exit velocity coefficient is 0.9825, indicating that the nozzle is highly efficient in converting the combustion chamber's energy into kinetic energy. At the nozzle exit, the static pressure is 1.17 x 105 Pa, and the exit temperature is 1165 K.

$$W(H,M,q) = \sqrt{2.\frac{\kappa g}{\kappa g - 1}.R.T9(H,M,q).\left[1 - \frac{1}{\left(\frac{P7(H,M,q)}{P9(H,M,q)}\right)^{\frac{\kappa g - 1}{\kappa g}}}\right]}$$

Equation 10: Equation for exit velocity

where:

- $W(H, M, q)$ is the exit velocity as a function of Altitude, Mach no and Air to fuel ratio
- $T9(H, M, q)$ is the static temperature at exit nozzle as a function of Altitude, Mach no and Air to fuel ratio
- $P7(H, M, q)$ is the pressure at exit nozzle as a function of Altitude, Mach no and Air to fuel ratio
- $P9(H, M, q)$ is the static pressure at exit nozzle as a function of Altitude, Mach no and Air to fuel ratio
- $\kappa g\ is\ gamma\ constant\ of\ gas$
- R is gas constant = 287

A pressure of 3.86 bar characterizes the nozzle inlet conditions, and a Mach number of 1.2 ensures the flow entering the nozzle is supersonic. The convergent-divergent nozzle design allows the flow to expand and further accelerate in the divergent section, reaching an exit Mach number of approximately 2.34 (calculated using the exit velocity and temperature).

3.6.4 Design Considerations

To ensure the nozzle can withstand the high temperatures and pressures experienced during operation, selecting appropriate materials and, if necessary, incorporating cooling methods is essential. Additionally, manufacturing constraints may need to be considered when designing the nozzle geometry to guarantee that the final product can be efficiently and reliably produced.

In conclusion, the convergent-divergent nozzle design for the 155mm ramjet-powered artillery shell is optimized to provide the necessary thrust for propelling the shell while ensuring efficient performance and durability under operational conditions.

4. Trajectory Generation in SIMULINK MATLAB

4.1 Introduction

The trajectory of a projectile plays a crucial role in determining the effectiveness and efficiency of artillery systems, particularly for long-range applications. Accurate trajectory prediction allows for better targeting, increased range, and improved overall performance of the artillery shell. In the context of the 155 mm ramjet-powered artillery shell, understanding its trajectory is essential for evaluating the benefits of incorporating a ramjet engine into the design and assessing the potential improvements in range and accuracy. A general 3DOF system is defined as:

$$d^2\ \frac{y_1}{dt^2} = f_1(t, y_1, y_2, y_3)$$
$$d^2\ \frac{y_2}{dt^2} = f_2(t, y_1, y_2, y_3)$$
$$d^2\ \frac{y_3}{dt^2} = f_3(t, y_1, y_2, y_3)$$

Equation 11: General 3DoF System of Equations

Where y_1, y_2, and y_3 are the degrees of freedom and f_1, f_2, and f_3 are functions of time t and the degrees of freedom.

The objectives of this trajectory analysis include the following:

- Predicting the flight path of the 155 mm ramjet-powered artillery shell using simplified trajectory equations
- Identifying key factors that influence the projectile's trajectory, such as aerodynamic coefficients, thrust profile, and initial conditions
- Analyzing the performance of the artillery shell in terms of range, maximum height, and time of flight

4.2 Trajectory Equations and Assumptions

To perform the trajectory analysis for the 155 mm ramjet-powered artillery shell, the following governing equations for projectile motion are used:

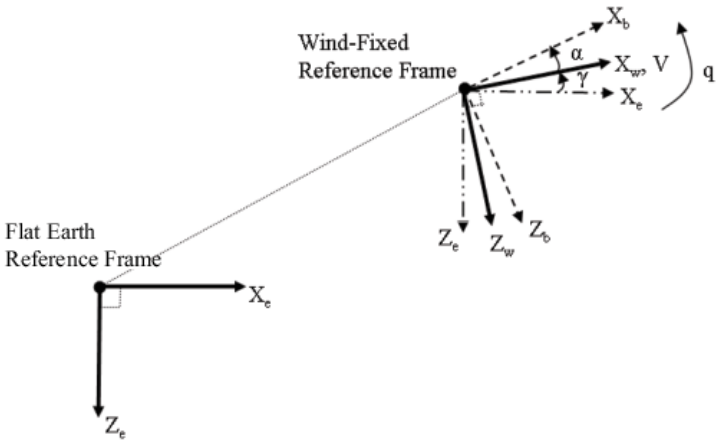

Figure 26 Frame of Reference in SIMULINK

$$A_{xb} = A_{xe} - qV \sin\alpha$$

$$A_{zb} = A_{ze} + qV \cos\alpha$$

$$A_{xe} = \left(\frac{F_x}{m} - g\ \sin\gamma\right)\cos\alpha - \left(\frac{F_z}{m} - g\ \cos\gamma\right)\ \sin\alpha$$

$$A_{ze} = \left(\frac{F_x}{m} - g\ \sin\gamma\right)\sin\alpha - \left(\frac{F_z}{m} - g\ \cos\gamma\right)\ \cos\alpha$$

$$V = \frac{F_x}{m} - g\ \sin\gamma$$

$$X_e = V\cos\gamma$$

$$Z_e = V\sin\gamma$$

$$q = \frac{M_y}{I_{yy}}$$

$$\gamma = q - \alpha$$

$$\alpha = \frac{F_z}{mV} + \frac{g}{V}\cos\gamma + q$$

Equation 12 : Equations of Motion

where for equation 14:

- A_{xb}: Lateral acceleration at point B
- A_{xe}: Lateral acceleration at point E
- A_{zb}: Vertical acceleration at point B
- A_{ze}: Vertical acceleration at point E
- V: Velocity of the vehicle
- α: Angle of attack (AOA)
- F_x: Lateral force acting on the projectile

- F_z: Vertical force acting on the projectile
- m: Mass of the projectile
- g: Acceleration due to gravity
- γ: Flight path angle
- X_e: Lateral position of point E
- Z_e: Vertical position of point E
- q: Pitch rate (angular projectile around the projectile's lateral axis)
- M_y: Yawing moment acting on the projectile
- I_{yy}: Moment of inertia around the projectile's yaw axis

To simplify the trajectory calculations, the following assumptions are made:

- The Earth is flat and non-rotating
- The atmosphere model of ISA is integrated
- A lookup table of the aerodynamic coefficients is integrated for the trajectory generation
- The projectile's mass remains constant throughout the flight; however, fuel mass is consumed during the flight time in the propulsion model
- The only external forces acting on the projectile are gravity and aerodynamic drag

These assumptions allow for a straightforward calculation of the projectile's trajectory while providing a reasonable approximation of the actual flight path.

4.3 Aerodynamic Coefficients and Drag Model

4.3.1 Aerodynamic Coefficients

For the 155 mm ramjet-powered artillery shell, the aerodynamic coefficients are provided as lookup tables. These tables contain values for the lift coefficient (C_L), drag coefficient (C_D), and pitching moment coefficient (C_m) as a function of the angle of attack (α) and Mach number (M). The use of lookup tables allows for an accurate and efficient representation of the shell's aerodynamic behavior throughout its flight.

4.3.2 Drag Model

In this study, no separate drag model is used. Instead, the drag coefficient (C_D) values provided in the lookup tables are directly used to compute the drag force acting on the artillery shell. The drag force (F_D) can be calculated using the following equation:

$$Drag\ Force = 0.5 \times \rho \times V^2 \times C_d \times S\_ref$$

Equation 13: Equation of Drag Force

where:

- ρ is the air density at a given altitude
- V is the velocity of the artillery shell
- C_D is the drag coefficient obtained from the lookup tables
- S_ref is the reference area, equal to 0.018136 m²

The trajectory analysis can account for the varying aerodynamic forces acting on the 155 mm ramjet-powered artillery shell throughout its flight by utilizing the aerodynamic coefficients and the drag model. This allows for a more accurate prediction of the shell's trajectory, performance, and range.

4.4 Trajectory Analysis and Simulation

4.4.1 Trajectory Simulation Methodology

A Simulink model using the Equations of Motion (EOM) block is employed for the trajectory analysis. The EOM block utilizes the ODE45, a variable time-step solver based on the Dormand-Prince pair of Runge-Kutta methods. This solver is chosen for its accuracy and efficiency in solving the system of ordinary differential equations (ODEs) that describe the motion of the artillery shell.

4.4.2 Environmental Conditions

The simulation considers the International Standard Atmosphere (ISA) model to account for variations in atmospheric properties with altitude. This model provides a standard representation of the Earth's atmosphere and is a basis for calculating aerodynamic forces acting on the artillery shell during flight.

4.4.3 Initial Conditions

The initial conditions for the simulation are as follows:

- Initial velocity: 684 m/s
- Launch angle: 44°
- Initial altitude: Sea level (0 m)

4.4.5 Simulation Constraints and Termination Conditions

The simulation is set to run for a user-defined time period, allowing for a customizable analysis of the artillery shell's flight path. This approach enables the user to examine the behavior of the artillery shell under various flight scenarios and determine the optimal conditions for maximizing its range and accuracy.

5. Results & Discussion

5.1 Trajectory Calculation Methodology

5.5.1 Trajectory Model

A 3-degrees of freedom (3-DOF) model is employed in this study to calculate the trajectory of the artillery shell. The 3-DOF model considers the translational motion in three axes (x, y, and z) while neglecting the rotational motion. This simplification is suitable for preliminary analysis and provides valuable insights into the system's performance.

5.5.2 Aerodynamic Forces and Moments

The aerodynamic forces and moments acting on the artillery shell are determined using lookup tables. These multidimensional arrays contain input values representing flight conditions, such as angle of attack, Mach number, and dynamic pressure, and output values representing the corresponding aerodynamic forces or moments. The aerodynamic coefficients can be accurately calculated for any given flight condition by interpolating between the given data points.

5.5.3 Thrust Profile

The thrust model starts providing thrust as soon as the shell leaves the muzzle. It burns 4.36 kg of fuel in 32 seconds, and the thrust varies from 523 N to 2004 N depending on the altitude and Mach number. This variation in thrust ensures that the shell maintains optimal performance throughout its flight. The thrust profile of the engine is tabulated below:

Table 5 Thrust Profile at Different Altitudes & Mach No

Time (s)	Mach No	Altitude (m)	Thrust Available (N)	Fuel Consumed (kg)
1.88	1.8	864	1900	0.9
6.88	2.05	3140	2004	0.9
11.88	2.24	5491	1880	0.83
16.88	2.39	7870	1510	0.68
21.88	2.41	10240	1120	0.5

26.88	2.39	12580	763	0.3
32.88	2.33	14890	523	0.25

5.5.4 Gravitational Force

The gravitational force acting on the artillery shell is accounted for in the 3-DOF model, affecting the vertical motion of the projectile.

5.5.5 Integration Method

The 4th-order Runge-Kutta method is used to integrate the equations of motion numerically. This solver offers a good balance between accuracy and computational efficiency, making it well-suited for trajectory calculations. The numerical solution for each degree of freedom y_i at time step h is calculated as follows:

$$\kappa 1_i = h \times f_i(t, y_1, y_2, y_3)$$

$$\kappa 2_i = h \times f_i\left(t + \frac{h}{2}, y_1 + \frac{k_{11}}{2}, y_2 + \frac{k_{12}}{2}, y_3 + \frac{k_{13}}{2}\right)$$

$$\kappa 3_i = h \times f_i\left(t + \frac{h}{2}, y_1 + \frac{k_{21}}{2}, y_2 + \frac{k_{22}}{2}, y_3 + \frac{k_{23}}{2}\right)$$

$$\kappa 4_i = h \times f_i\left(t + \frac{h}{2}, y_1 + \frac{k_{31}}{2}, y_2 + \frac{k_{32}}{2}, y_3 + \frac{k_{33}}{2}\right)$$

$$y_i = y_i + \left(\frac{1}{6}\right) \times (\kappa 1_i + 2k2_i + 2k3_i + 2k3_i + k4_i)$$

Equation 14: 4th-order Runge-Kutta Method

With this methodology, the trajectory of the 155mm ramjet-powered artillery shell can be analyzed under various flight conditions, providing valuable insights into the system's performance and potential improvements.

5.2 Trajectory Analysis

The performance analysis of the 155mm ramjet-powered artillery shell showcases a remarkable improvement in range and altitude compared to conventional artillery systems. The maximum range achieved in our simulations is 70 km, while the apogee reaches 14 km. The integration of

the ramjet engine plays a pivotal role in these enhanced capabilities, providing sustained thrust throughout the flight.

The convergent-divergent nozzle design is optimized to maintain high exit velocity while adapting to varying pressure conditions. As the altitude increases, the thrust decreases due to the decrease in dynamic pressure, which affects the nozzle performance. This, in turn, ensures an efficient propulsion system that enables the shell to maintain its high speed and reach extended ranges. The combustion chamber's design and operation also contribute to the performance by providing an optimal combustion process that maintains high temperatures and pressures.

The graphical representations in Figure 26 below of the trajectory simulations, including plots of range, altitude, angle of attack, pitching angle, thrust, flight path angle, velocity, Mach no, total mass & fuel mass versus time, further support our analysis and demonstrate the key factors contributing to the enhanced performance of the 155mm ramjet-powered artillery shell. Overall, the innovative design and integration of the ramjet engine, combined with the optimized nozzle and combustion chamber, resulted in a significantly increased range and altitude, offering a substantial advantage in modern warfare scenarios.

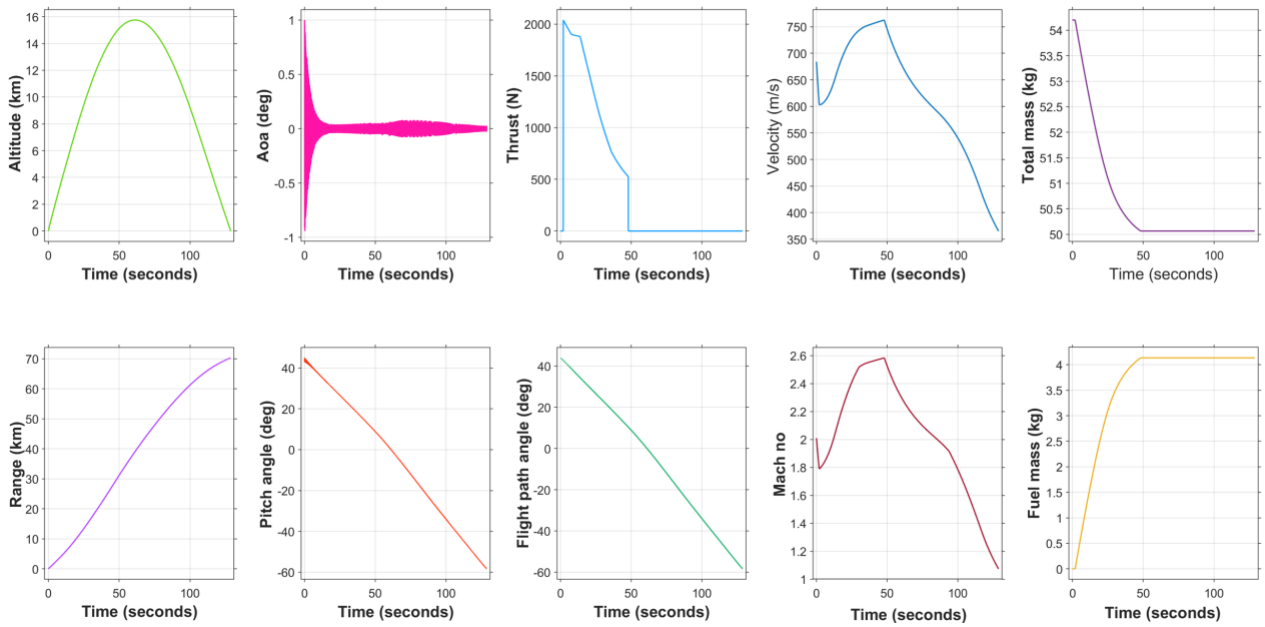

Figure 27 Powered Shell Output Graphs

5.3 Comparison with Conventional Artillery Systems

By incorporating a ramjet engine and optimizing the propulsion system, our analysis demonstrates a significant performance improvement compared to conventional artillery systems, as shown in the figure below.

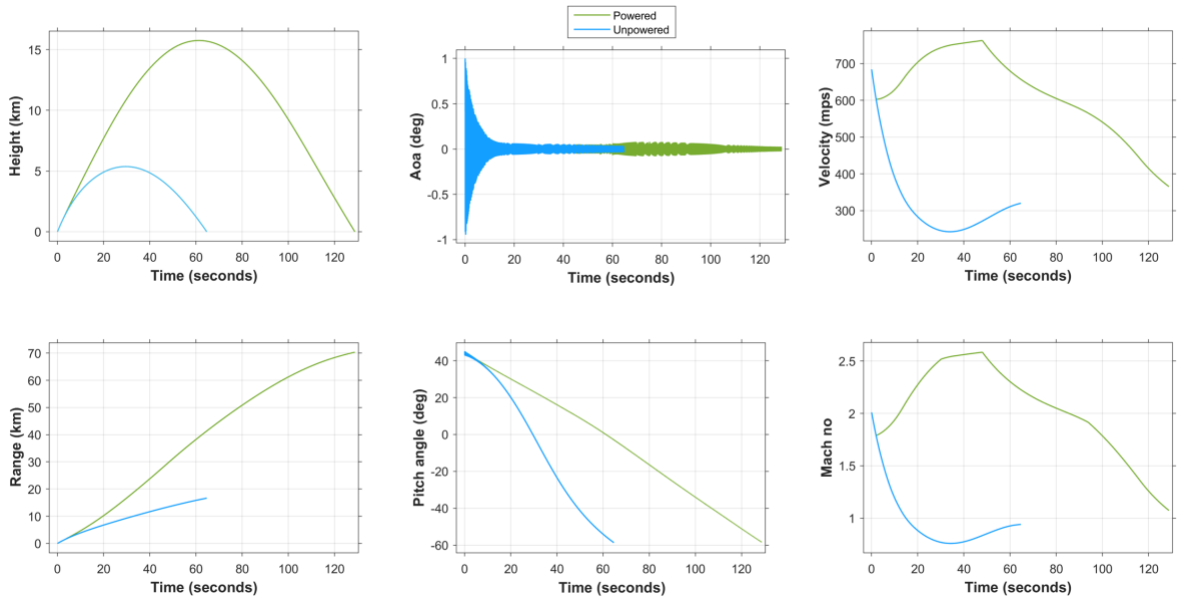

Figure 28 Powered vs. Unpowered Comparison Graphs

In Figure 28 above, it can be seen very clearly that the Apogee is increased from 5 km to 16 km after the integration of the propulsion system, and the overall effect on the range is from 16 km to 70 km, which is a remarkable increase in the range as compared to the traditional artillery shell.

6.0 Potential Improvements and Future Work

While the results obtained from the current study are promising, there are several areas in which further research and development can lead to enhanced performance and capabilities for the 155mm ramjet-powered artillery shell. This section discusses potential improvements and future work that can be explored.

6.1 Engine Optimization

Further optimization of the ramjet engine can improve efficiency, thrust, and overall performance. This may include refining the combustion chamber design, improving the fuel injection method, and optimizing the nozzle geometry. Additionally, more advanced computational fluid dynamics (CFD) simulations can be employed to understand the flow dynamics within the engine better and identify potential areas for improvement.

6.2 Guidance and Control Systems

Integrating advanced guidance and control systems can significantly enhance the accuracy and effectiveness of the artillery shell. By incorporating technologies such as GPS, FOG-based inertial navigation systems, or other advanced guidance methods, the shell can be precisely guided to its target. Additionally, incorporating active control surfaces and adaptive algorithms can help to maintain stability and improve maneuverability during flight, allowing for more effective engagement of dynamic targets.

6.3 Advanced Materials and Manufacturing Techniques

The use of advanced materials and manufacturing techniques can significantly improve the structural integrity, weight, and overall performance of the artillery shell. Lightweight, high-strength materials can reduce the overall mass of the shell, allowing for increased payload capacity and improved range. Furthermore, advancements in manufacturing techniques, such as additive manufacturing or composite material fabrication, can lead to more efficient and cost-effective production of artillery shells, making them more accessible for widespread use in military operations.

In conclusion, this study has demonstrated the potential of a ramjet-powered 155mm artillery shell to improve range and altitude performance significantly. However, there are still numerous areas for potential improvement and future research that can further enhance the capabilities of this promising technology. By continuing to explore these opportunities, developing more effective and efficient artillery systems can contribute to advancing modern warfare capabilities.

Bibliography

[1] J. Kinard, Artillery An Illustrated History Of Its Impact, ABC-CLIO, 2007.

[2] J. Grace, "GPS Guidance, Digital Fire Control Systems, And Advanced Ammunition," *IEEE Aerospace And Electronic Systems Magazine*, Vol. 15, No. 6, Pp. 15-17, 2000.

[3] R. C. B. Howard J. Gibeling, "Projectile Base Bleed Technology Part I: Analysis And Results," Scientific Research Associates, Inc. , 50 Nye Road P.O. Box 1058 Glastonbury, CT 06033, 1992.

[4] S. C. &. W. T. A. (. Perkins, "Design Of An Artillery Projectile With A Ramjet For Extended Range," *Journal Of Spacecraft And Rockets*, Vol. 47, No. 1, Pp. 144-152.

[5] M. A. R. U. &. A. A. A. Hamidullah, "Artillery Ammunition: A Technological Review.," *Defence Science Journal*, Vol. 65, No. 3, Pp. 243-251, 2015.

[6] T. J. &. H. I. V. Gander, Jane's Ammunition Handbook, Jane's Information Group, 1993.

[7] ,. M. F. LEMOS, A. P. D. SILVA, P. S. T. AMARAL, ,. E. D. S. SOUZA, ,. L. J. D. S. Jãºnior, R. C. PINTO, W. K. D. O. FERREIRA, K. DE OLIVEIRA And V., "FROM BENCH TO SHOOTING RANGE: CORRELATING BASE BLEED CHEMISTRY WITH THE BALLISTIC PERFORMANCE OF EXTENDED RANGE MUNITION," In *32ND INTERNATIONAL SYMPOSIUM ON BALLISTICS*, 2022.

[8] D. Ashoke And P. Chettri, "Drag Reduction With Optimum Designing Of A Base Bleed Projectile Using Computational Analysis.," *Nnovations In Sustainable Energy And Cleaner Environment*, Pp. 23-45., 2020.

[9] H. A. Abou-Elela, A. Z. Ibrahim, O. K. Mahmoud And O. E. Abdel-Hamid., "EFFECT OF BASE BLEED DIMENSIONS ON THE BALLISTIC PERFORMANCE OF ARTILLERY PROJECTILES.," In *The International Conference On Applied Mechanics And Mechanical Engineering*,, 2014.

[10] . H. A. Abou-Elela, . A. Z. Ibrahim, O. K. Mahmoud And O. E. Abdel-Hamid, "Ballistic Analysis Of A Projectile Provided With Base Bleed Unit.," In *International Conference On Aerospace Sciences And Aviation Technology*., 2013.

[11] N. Kubberud And I. J. Oye, "Extended Range Of 155mm Projectile Using An Improved Base Bleed Unit. Simulations And Evaluation.," In *26th International Symposium On Ballistics.*, 2011.

[12] N. E. A. K. &. H. R. Gunners, "Base-Bleed Systems For Gun Projectiles.," *Progress In Astronautics & Aeronautics*, Vol. 100, No. 27, 1988.

[13] J. E. Danberg, "Analysis Of The Flight Performance Of The 155 Mm M864 Base Burn Projectile.," In *ARMY BALLISTIC RESEARCH LAB ABERDEEN PROVING GROUND MD*, 1990.

[14] J.-S. Hwang And C.-K. Kim, "Structure And Ballistic Properties Of K307 Base Bleed Projectile," In *16th Int. Sympo. On Ballistics*, California, USA,, 1996.

[15] V. Schabort And P. Karsten, "Toward A Better Base-Bleed," In *18th Int. Sympo. On Ballistics*, Texas, USA, 1999.

[16] H. A. Abou-Elela, , A. Z. Ibrahim, . O. K. Mahmoud And O. E. Abdel-Hamid, "The Optimization Of Base Bleed Grain Parameters For Maximum Ballistic Performance," In *International Conference On Aerospace Sciences And Aviation Technology*, 2015.

[17] E. M. Youssef, T. Elshenawy, H. E. Mostafa, . M. Radwan And A. Elbeih, "Optimization Of Low Signature Base Bleed Propellant Formulations.," In *Nternational Conference On Aerospace Sciences And Aviation Technology*, 2019.

[18] T. Mathur, And J. C. Dutton, "Base-Bleed Experiments With A Cylindrical Afterbody In Supersonic Flow.," *Ournal Of Spacecraft And Rockets*, Vol. 33, No. 1, Pp. 30-37, 1996.

[19] D. Regodić, A. Jevremović And D. Jerković, "The Prediction Of Axial Aerodynamic Coefficient Reduction Using Base Bleed," *Aerospace Science And Technology* , Vol. 31, No. 1, Pp. 24-29., 2013.

[20] P. A. O. G. Korting, F. W. M. Zee And J. J. Meulenbrugge, "Combustion Characteristics Of Low Flame Temperature, Chlorine-Free Composite Solid Propellants.," *Journal Of Propulsion And Power,*, Vol. 6, No. 3, Pp. 250-255, 1990.

[21] B. L. Tozer, "Rocket Assisted Projectile (RAP) Development Program," *5 Inch/38 Safety Test Program.*, Vol. Part 4, 1970.

[22] J.-Y. Jeong And S.-H. Choi, "Propellant Characteristics Used For A Rocket-Assisted Projectile With Aluminium Contents," *Journal Of The Korean Society Of Propulsion Engineers*, Vol. 23, No. 5, 2019.

[23] V. Arkhipov And K. Perfilieva, "Optimization Of Construction Of The Rocket-Assisted Projectile," In *MATEC Web Of Conferences.*, 2017.

[24] M. S. Nawwar, T. Z. Wafy And H. E. Mustafa, "Performance Of Composite Solid Rocket Propellants For Rocket Assisted Projectiles (RAP).," In *He International Conference On Chemical And Environmental Engineering.*, 2016.

[25] R. X. Meyer, "In-Flight Formation Of Slag In Spinning Solid Propellant Rocket Motors," *Ournal Of Propulsion And Power*, Vol. 8, No. 1, Pp. 45-50, 1992.

[26] K.-M. Kim, J.-H. Cho And D.-J. Jeong, "혼합형 고체추진제의 RAP (Rocket Assisted Projectile) 적용연구; 혼합형 고체추진제의 RAP (Rocket Assisted Projectile) 적용연구; Study On Composite Solid Propellants For Rocket Assisted Projectile.," *Ournal Of The Korean Society For Aeronautical & Space Sciences* , Vol. 38, No. 11, Pp. 1081-1086, 2010.

[27] H. Saidpour, M. Razmara And S. Arunachalam, "DMA Investigation On Polyurethane," In *Nternational Conference On Fascinating Advancement In Mechanical Engineering* , 2008.

[28] M. Niehaus And O. Greeb, "Optimization Of Propellant Binders–Part Two: Macroscopic Investgation Of The Mechanical Properties Of Polymers.," *Propellants, Explosives, Pyrotechnics: An International Journal Dealing With Scientific And Technological Aspects Of Energetic Materials* , Vol. 29, No. 6, Pp. 333-338, 2004.

[29] Ö. Hocaoğlu, T. Özbelge, F. Pekel And S. Özkar, "Fine-Tuning The Mechanical Properties Of Hydroxyl-Terminated Polybutadiene/Ammonium Perchlorate-Based Composite Solid Propellants By Varying The NCO/OH And Triol/Diol Ratios.," *Journal Of Applied Polymer Science*, Vol. 84, No. 11, Pp. 2072-2079, 2002.

[30] S. F. Zawadzki And L. Akcelrud, "HTPB-Based Polyurethanes: A Correlation Study Between Morphology And Mechanical Behaviour.," *Polymer International* , Vol. 42, No. 4, Pp. 422-428, 1997.

[31] S. Benli, Ü. Yilmazer, F. Pekel And S. Özkar, "Effect Of Fillers On Thermal And Mechanical Properties Of Polyurethane Elastomer.," *Journal Of Applied Polymer Science*, Vol. 68, No. 7, Pp. 1057-1065, 1998.

[32] P. A. Kakavas, "Mechanical Properties Of Propellant Composite Materials Reinforced With Ammonium Perchlorate Particles.," *International Journal Of Solids And Structures*, Vol. 51, No. 10, Pp. 2019-2026, 2014.

[33] Z. Mehmood And M. B. Khan, "Synergistic Enhancement In Mechanical And Ballistic Properties Of HTPB Based Energetic Polymer Composites.," *Plastics, Rubber And Composites* , Vol. 42, No. 10, Pp. 446-452, 2013.

[34] M. S. Nawwar, T. Z. Wafy And H. E. Mustafa, "Performance Of Composite Solid Rocket Propellants For Rocket Assisted Projectiles (RAP).," *The International Conference On Chemical And Environmental Engineering.*, Vol. 8, No. 8, 2016.

[35] J. E. Danberg, "Analysis Of The Flight Performance Of The 155 Mm M864 Base Burn Projectile.," *ARMY BALLISTIC RESEARCH LAB ABERDEEN PROVING GROUND MD*, 1990.

[36] E. K. Bastress , "Interior Ballistics Of Spinning Solid-Propellant Rockets.," *Journal Of Spacecraft And Rockets* , Vol. 2, No. 3, Pp. 455-457, 1965.

[37] R. P. Ayerst And B. G. Tucker, "Improvements In Tensile Testing Of Composite Propellants.," In *EXPLOSIVES RESEARCH AND DEVELOPMENT ESTABLISHMENT WALTHAM ABBEY*, 1971.

[38] S. Kang, C. Park, W. Jung And T. Kwon, "Kang, Shinjae, Et Al. "Design Of Gun Launched Ramjet Propelled Artillery Shell With Inviscid Flow Assumption," *Journal Of The Korean Society Of Propulsion Engineers*, Vol. 19, No. 4, Pp. 52-60, 2015.

[39] L. Wang, Z. Wu, H. Chi, C. Liu, H. Tao And Q. Wang, "Numerical And Experimental Study On The Solid-Fuel Scramjet Combustor.," *Journal Of Propulsion And Power* , Vol. 31, No. 2, Pp. 685-693, 2015.

[40] . L. Biao, Z. Wei And H. Chi, "Numerical Analysis Of Solid Fuel Scramjet Operating At Mach 4 To 6.," In *49th AIAA/ASME/SAE/ASEE Joint Propulsionconference*, 2013.

[41] B. Kert, V. Hubasov, E. Znamensky, V. Kravtsov, Y. Pavlov, A. Panchenko And Y. Genkin, "Ballistic Opportunities' Evaluation Of Artillery Projectile With A Rocket Ramjet.," *Physical-Chemical Kinetics In Gas Dynamics*, Vol. 20, No. 2, 2019.

[42] F. S. B. E. I. O. H. P. E. ". S. U. (Tulgu), "АКТИВНО-РЕАКТИВНЫЙ СНАРЯД.". Russia Patent RU 2493533 C1, 20 September 2013.

[43] T. S. U. (Tulsu), "METHOD FOR INCREASING FLIGHT RANGE OF ARTILLERY SHELL AND DEVICE FOR ITS IMPLEMENTATION". Russia Patent RU 2251068 C1 , 25 April 2005.

[44] F. S. B. E. I. O. H. P. E. ". S. U. (Tulgu), "METHOD FOR INCREASING FLIGHT RANGE OF ARTILLERY SHELL AND DEVICE FOR ITS IMPLEMENTATION". Russia Patent RU 2486452 C1, 27 June 2013.

[45] Y. L. S. ,. K. V. A. ,. S. E. V. ,. S. M. S. ,. F. V. D. ,. F. V. P. ,. Z. N. P. ,. A. V. SOROKIN VLADIMIR ALEKSEEVICH, "ROCKET-DIRECT-FLOW ENGINES ON SOLID AND PASTE FUELS". Russia Patent 629.7.036.22.001(024), 2010.

[46] F. S. S. M. E. I. O. H. E. ". T. G. M. A. O. T. S. M. F. O. T. M. O. D. O. T. R. Federation, "METHOD FOR PREPARING COLLOID PASTE". Russia Patent RU 2637330 C , 12 April 2017.

[47] He, Yongpan,, Y. Chen, D. Liu, J. Liu, M. Lai And X. Liang, "Research On Solid Rocket/Scramjet Combined Engine.," In *1st AIAA International Space Planes And Hypersonics Technologies Conference*, 2017.

[48] V. Yogeshkumar, N. Rathi And P. A. Ramakrishna, "Solid Fuel-Rich Propellant Development For Use In A Ramjet To Propel An Artillery Shell.," *Defence Science Journal* , Vol. 70, No. 3, 2020.

[49] S. Verma And P. A. Ramakrishna., "Effect Of Specific Surface Area Of Aluminum On Composite Solid Propellant Burning," *Journal Of Propulsion And Power* , Vol. 29, No. 5, Pp. 1200-1206, 2013.

[50] M. Gaurav And P. A. Ramakrishna, "Effect Of Mechanical Activation Of High Specific Surface Area Aluminium With PTFE On Composite Solid Propellant," *Combustion And Flame*, Vol. 166, Pp. 203-215, 2016.

[51] K. Ishitha And P. A. Ramakrishna, "Activated Charcoal: As Burn Rate Modifier And Its Mechanism Of Action In Non-Metalized Composite Solid Propellants.," *Nternational Journal Of Advances In Engineering Sciences And Applied Mathematics*, Vol. 6, Pp. 76-96, 2014.

[52] J. Benacka, "Introduction To 3D Graphics Through Excel.," *Informatics In Education-An International Journal*, Vol. 12, No. 2, Pp. 221-230, 2013.

[53] J. Benacka, "Spreadsheet Numerical Modeling In Secondary School Physics And Biology.," *Spreadsheets In Education*, Vol. 2, No. 3, 2008.

[54] J. Benacka, "Projectile General Motion In A Vacuum And A Spreadsheet Simulation," *Physics Education*, Vol. 50, No. 1, P. 58, 2014.

[55] J. Benacka, "Creating Realistic 3D Graphics With Excel At High School-Vector Algebra In Practice," *Informatics In Education-An International Journal* , Vol. 14, No. 2, Pp. 161-173, 2015.

[56] J. Benacka And I. Stubna, "Ball Launched Against An Inclined Plane–An Example Of Using Recurrent Sequences In School Physics," *Nternational Journal Of Mathematical Education In Science And Technology*, Vol. 40, No. 5, Pp. 696-705, 2009.

[57] J. Benacka And S. Ceretkova, "Excel Modelling In Upper Secondary Mathematics–A Few Tips For Learning Functions And Calculus.," *Proceedings Of CERME,* Vol. 8, Pp. 970-979, 2013.

[58] J. Benacka And S. Ceretkova, "Modelling Harvesting Animal Population At High School With Spreadsheets–The Case Of Moby Dick," *Spreadsheets In Education,* Vol. 7, No. 3, P. 9, 2014.

[59] T. Brosnan, "Using Spreadsheets To Develop Understanding In Science.," *Learning Within Artificial Worlds,* Pp. 76-84, 2013.

[60] S. Crook, M. Sharma And R. Wilson, " An Evaluation Of The Impact Of 1: 1 Laptops On Student Attainment In Senior High School Sciences.," *Nternational Journal Of Science Education,,* Vol. 37, No. 2, Pp. 272-293, 2015.

[61] J. Benacka, "High-Altitude Free Fall Revised," *High-Altitude Free Fall Revised.,* Vol. 78, No. 6, Pp. 616-619, 2010.

[62] J. Benacka, "Numerical Modelling With Spreadsheets As A Means To Promote STEM To High School Students.," *EURASIA Journal Of Mathematics, Science And Technology Education,* Vol. 12, No. 4, Pp. 947-964, 2016.

[63] V. V. Chistyakov, "On One Numerical Method Of Integrating The Dynamical Equations Of Projectile Planar Flight Affected By Wind.," *Discrete And Continuous Models And Applied Computational Science,* Vol. 3, Pp. 125-137, 2014.

[64] D. Klatt, M. Proff And R. Hruschka, "Investigation Of The Flight Behavior Of A Flare-Stabilized Projectile Using 6dof Simulations Coupled With CFD.," *International Journal Of Numerical Methods For Heat & Fluid Flow* , Vol. 30, No. 9, Pp. 4185-4201, 2019.

[65] W. Yu And X. Zhang, "Aerodynamic Analysis Of Projectile In Gun System Firing Process.," *Journal Of Applied Mechanics,* Vol. 77, No. 5, 2010.

[66] Z. ZHANG, C. MENG And Y. WANG, "Six-Dimensional Ballistics Of A Certain Howitzer Projectile Considered With Dynamic Unbalance.," In *31st International Symposium On Ballistics*, 2019.

[67] P. A. P. C. Hill, Mechanics And Thermodynamics Of Propulsion, New York: Addison-Wesley, 1992.

[68] W. H. H. A. D. T. P. Jack D. Mattingly, Aircraft Engine Design, 2002.

[69] G. P. S. A. O. Biblarz, Rocket Propulsion Elements, John Wiley & Sons, 2016.

[70] Y. P. R. Ya B. Zel'dovich, Physics Of Shock Waves And High-Temperature Hydrodynamic Phenomena, Courier Corporation, 2002.

[71] J. John D. Anderson, INTRODUCTION TO FLIGHT, New York: Mcgraw-Hill Book Company, 1989.

[72] W. H. M. S. A. M. A. D. R. M. R. M. Cummings, Applied Computational Aerodynamics: A Modern Engineering Approach, Cambridge University Press, 2015.

[73] D. P. D. D. A. U. M. William Heiser, Hypersonic Airbreathing Propulsion, AIAA Education Series, 1994.

[74] M. N. B. A. S. M. II'yashenko, RAMJET ENGINES, Oosudarstvennoyo Izdatel'stvo Oboronnoy Promyshlennosti, 1960.

[75] J. D. B. G. B. R. Oosthuizen1, "SOLID FUEL RAMJET (SFRJ) PROPULSION FOR ARTILLERY PROJECTILE APPLICATIONS – CONCEPT DEVELOPMENT OVERVIEW," *International Symposium Of Ballistics,* 2001.

[76] J.-K. Fu, And S.-M. Liang, "Drag Reduction For Turbulent Flow Over A Projectile: Part I," *Journal Of Spacecraft And Rockets,* Vol. 31, No. 1, Pp. 85-92., 1994.

[77] Y.-K. Lee, H.-D. Kim And S. Raghunathan, "Optimization Of Mass Bleed For Base-Drag Reduction," *AIAA Journal,* Vol. 45, No. 7, Pp. 1472-1477., 2007.

[78] M. A. Lau And S. J. Sugden, "Applications Of Spreadsheets In Education: The Amazing Power Of A Simple Tool.," 2011.

[79] M. Keune And H. Henning, "Modelling And Spreadsheet Calculation," *Mathematical Modelling In Education And Culture,* Pp. 101-110., 2003.

Annexure

Atmospheric data:

Design Mach Angles for Mach 3.2 and respective cone angle

$$\alpha 1d200 = 3.0256 - 2.8650Md + 1.3085Md^2 - 0.2797Md^3 + 0.02299Md^4$$
$$\alpha 1d225 = 3.1855 - 3.0444Md + 1.4062Md^2 - 0.30282Md^3 + 0.02501Md^4$$
$$\alpha 1d250 = 4.4295 - 4.9385Md + 2.5051Md^2 - 0.5811Md^3 + 0.0510Md^4$$
$$\alpha 1d275 = 3.7634 - 3.7497Md + 1.7831Md^2 - 0.3915Md^3 + 0.03280Md^4$$
$$\alpha 1d300 = 4.3144 - 4.4707Md + 2.1686Md^2 - 0.48273Md^3 + 0.04084Md^4$$

Equations of Pressure Recovery in first cone shock wave:

$$dSR200 = 0.01015 - 0.11587M + 0.03485M^2$$
$$dSR225 = 0.118433 - 0.142761M + 0.04629M^2$$
$$dSR250 = 0.118723 - 0.156566M + 0.05626M^2$$
$$dSR275 = 0.124400 - 0.172760M + 0.06728M^2$$
$$dSR300 = 0.115713 - 0.1754038M + 0.07619M^2$$